Journal of Medicinal Chemistry

Article

Modeling, Synthesis and Biological Evaluation of Potential Retinoid-X-Receptor (RXR) Selective Agonists: Analogs of 4-[1-(3,5,5,8,8-Pentamethyl-5,6,7,8-tetrahydro-2-naphthyl)ethynyl]benzoic Acid (Bexarotene) and 6-(ethyl(5,5,8,8-tetrahydronaphthalen-2-yl)amino)nicotinic Acid (NEt-TMN)

Michael C Heck, Carl Edward Wagner, Pritika H. Shahani, Mairi MacNeill, Aleksandra Grozic, Tamana Darwaiz, Micah Shimabuku, David G Deans, Nathan M Robinson, Samer H Salama, Joseph W. Ziller, Ning Ma, Arjan van der Vaart, Pamela A. Marshall, and Peter W. Jurutka

J. Med. Chem., **Just Accepted Manuscript** • DOI: 10.1021/acs.jmedchem.6b00812 • Publication Date (Web): 03 Sep 2016

Just Accepted

ACS Publications

Journal of Medicinal Chemistry is published by the American Chemical Society. 1155 Sixteenth Street N.W., Washington, DC 20036

Modeling, Synthesis and Biological Evaluation of Potential Retinoid-X-Receptor (RXR) Selective Agonists: Analogs of 4-[1-(3,5,5,8,8-Pentamethyl-5,6,7,8-tetrahydro-2-naphthyl)ethynyl]benzoic Acid (Bexarotene) and 6-(ethyl(5,5,8,8-tetrahydronaphthalen-2-yl)amino)nicotinic Acid (NEt-TMN)

*Michael C. Heck[1], Carl E. Wagner[1], Pritika H. Shahani, Mairi MacNeill, Aleksandra Grozic, Tamana Darwaiz, Micah Shimabuku, David G. Deans, Nathan M. Robinson, Samer H. Salama, Joseph W. Ziller[§], Ning Ma[‡], Arjan van der Vaart[‡], Pamela A. Marshall, Peter W. Jurutka**

School of Mathematical and Natural Sciences, New College of Interdisciplinary Arts and Sciences, Arizona State University, 4701 W. Thunderbird Road, Glendale, AZ 85306.

[§]Department of Chemistry, University of California, Irvine, 576 Rowland Hall, Irvine, CA 92697

[‡]Department of Chemistry, University of South Florida, 4202 E Fowler Ave, CHE 205, Tampa, FL, 33620.

[1] These authors contributed equally to this work.

ABSTRACT Sulphonic acid analogs of 4-[1-(3,5,5,8,8-pentamethyl-5-6-7-8-tetrahydro-2-naphthyl)ethynyl]benzoic acid (**1**)—or bexarotene—as well as seven novel and two reported analogs of 6-(ethyl(5,5,8,8-tetramethyl-5,6,7,8-tetrahydronaphthalen-2-yl)amino)nicotinic acid (**NEt-TMN**) were synthesized and assessed for selective retinoid-X-receptor (RXR) agonism. Compound **1** is FDA-approved for treatment of cutaneous T-cell lymphoma (CTCL); however, **1** can provoke side-effects by impacting RXR-dependent receptor pathways. All analogs in this study were evaluated for their potential to bind RXR through modeling and then assayed in an RXR-RXR mammalian-2-hybrid (M2H) system and in RXRE-mediated transcriptional experiments. The EC_{50} profiles for these unique analogs, and their analogous effectiveness to inhibit proliferation in CTCL cells compared to **1**, suggest these compounds possess similar or even enhanced therapeutic potential. Several compounds also displayed more selective RXR activation with minimal cross-signaling of the retinoic-acid-receptor. These results suggest that modifications of potent RXR agonists such as **NEt-TMN** can lead to improved biological selectivity and potency compared to the known therapeutic.

Introduction

There are three known isoforms (α, β, γ)[1] of the human retinoid X receptors (hRXRs), with one or more being expressed in every human tissue type, that primarily function as versatile transcription factors. The RXRs often act as heterodimeric partners with other receptors of the nuclear receptor (NR) superfamily comprising transcriptional regulators that include the retinoic acid receptor (RAR), the thyroid hormone receptor (TR), the peroxisome proliferator-activated receptor (PPAR), the vitamin D receptor (VDR), and the liver X receptor (LXR), to name only a few. All nuclear receptors modulate gene expression, generally promoting transcription, when signaled by a specific receptor ligand. This ligand, often a natural endogenous molecule, associates with the receptor by binding to a receptor ligand-binding domain (LBD) precipitating a conformational change that permits high affinity receptor binding to the receptor's corresponding hormone responsive element (HRE) on the DNA. While HREs have increasingly been located either up- or downstream a considerable distance from the genes they regulate, many HREs have been found close to or within the regulated gene promoter region. The HREs exhibit sequence specificity, typically consisting of two hexad repeat sequences made up of half-sites punctuated by a variable number of nucleotide spacers between these inverted, direct or everted repeats.[2] The corresponding HREs for VDR, TR and RAR, contain half-sites separated with 3, 4, and 5 nucleotide spacers, respectively.[3]

While VDR, TR and RAR were first believed to bind as homodimers to their corresponding HREs[4], they actually partner with RXR to form heterodimers in order to bind to their HREs.[5] When one of several natural RXR agonist ligands such as 9-*cis*-retinoic acid (9-*cis*-RA) binds to RXR, an RXR homodimer self-assembles that then binds to RXR responsive elements (RXREs). When RXR partners with other NRs in heterodimers, it does so either with

bound or unbound ligand within the RXR LBD. With respect to the RXR-VDR heterodimer, RXR has been reported to be unoccupied.[6] Alternatively, evidence suggests that RXR possesses a ligand to function as a RXR:LXR heterodimer.[7] Considering this versatility, it is not surprising that RXR has been classified as the primary NR regulator, since it is often a prerequisite for heterodimer formation and proper transcriptional activation of other NRs corresponding response elements.[8]

A multitude of studies employing rexinoids, RXR and a variety of different nuclear receptors, have resulted in two primary classifications for RXR-heterodimer complexes—namely permissive and nonpermissive heterodimers. Only ligands selective for the RXR partner can activate purely nonpermissive RXR heterodimers, whereas either RXR specific ligands or the partner-selective ligands can activate permissive RXR heterodimers.[9] The generally nonpermissive RXR heterodimers include RXR-VDR, RXR-RAR and RXR-TR. In most (but not in all) circumstances, RXR is "silent" in VDR and TR heterodimers. The RXR-RAR heterodimer, however, shows increased activity with select RXR agonists in combination with an RAR ligand. In fact, a few rexinoids have been reported to stimulate RXR-RAR, despite the absence of a RAR-specific ligand.[10] In this respect, RXR-RAR has been termed conditionally nonpermissive. Finally, the RXR-PPARs, RXR-LXRs, and RXR-FXR heterodimers have been observed to be fully permissive.

Developing RXR-specific agonists for clinical therapeutic treatments is complicated not only by potential pleiotropic effects arising from the activation of permissive RXR heterodimers, but also from a limited RXR pool that may be titrated away from RXR-containing heterodimers to instead form RXR homodimers in certain cell conditions and tissue types—thereby limiting the ability of the nonpermissive RXR heterodimers to form and function. For instance, RXR

agonists such as 9-cis RA can arrest nonpermissive heterodimer activation in VDR[11] or TR.[12] Moreover, NR agonists like T3 or 1,25-dihydroxyvitamin D_3 (1,25D) that promote RXR heterodimer formation with TR and VDR, respectively, may also drive crosstalk inhibition of other RXR-dependent receptors utilizing the limited RXR pool. In fact, this crosstalk inhibition has been observed for T_3-TR-RXR-directed inhibition of VDR transactivation[13] as well as 1,25D-VDR-RXR-mediated inhibition of TR function[14, 12]; however, the cross-receptor squelching mechanism likely extends further than simple RXR sequestration. Nevertheless, two key issues in developing therapeutic rexinoids with decreased pleiotropic effects concern RXR potency and heterodimer selectivity. Hence, an approach to modify the structure of the central RXR heterodimer agonist may lead to specific NR modulators (SNuRMs) that exhibit unique characteristics arising from varying NR control.[15]

Selective RXR ligand (rexinoid) SNuRMs are attractive medicinal drug targets because activating RXR selectively versus RAR bestows chemotherapeutic effects in an array of human cancer types without incurring toxicities arising from RAR crossover.[16] Following lengthy development and testing[17] of 9-*cis* RA modeled compounds, 4-[1-(3,5,5,8,8-pentamethyltetralin-2-yl)ethynyl]benzoic acid (**1**)[18] was demonstrated to possesses high RXR agonist specificity, and Ligand Pharmaceuticals Inc. eventually gained FDA approval for the drug, more commonly called bexarotene, for cutaneous T-cell lymphoma (CTCL) treatment. Many structurally similar bexarotene analogs, like disilabexarotene (**2**)[19], have been reported over the last twenty years and many of these rexinoids possess RXR specific agonism similar to bexarotene.

Figure 1

While bexarotene (**1**) was approved as a treatment for CTCL, it has been explored for therapeutic effects in colon cancer[20], mammary carcinoma[21] and a proof-of-concept (POC)

clinical trial has shown it effective in non-small cell lung cancer[22], since the up-regulation of certain RXR-controlled genes suppresses cell proliferation while synergizing apoptosis in cancer cells subjected to chemotherapuetics.[20] Several rexinoids, following compound **1**, were investigated in non-insulin-dependent diabetes mellitus (NIDDM) mouse models, because the RXR:PPAR heterodimer impacts metabolism.[23] Despite bexarotene's RXR-specificity versus RAR, its known side-effects include hypothyroidism[24], hyperlipidemia, and cutaneous toxicity. Like 9-*cis*-RA, side-effects of bexarotene arise from disrupting nonpermissive receptor activation, as in TR[25] resulting in hypothyroidism, or stimulating permissive receptor activation, as in LXR leading to hyperlipidemia[26] or in RAR effecting cutaneous toxicity[27] with therapeutic dose concentrations. Hence, the approach to design, model and synthesize more potent and selective rexinoids whose pleiotropic effects are attenuated is active area of research. Adding to the motivation to create novel rexinoids, RXR selective agonists have recently been investigated in neurodegenerative diseases such as Parkinson's disease[28], and a recent POC trial of bexarotene in patients with mild to moderate Alzheimer's disease (AD)—driven by controversial murine studies in AD[29]—revealed provocative results in critical human biomarkers in the clinic.[30]

Many RXR specific ligands modeled after 9-*cis* RA and **1** have been reported. For instance, the cyclopropyl-dienoic acid (**3**)[31] has been shown to be more potent as an RXR agonist than its enantiomer. The 9cUAB30 (**4**)[32] is in advanced clinical trials for breast cancer[33], and many 9cUAB30 analogs[34] have also been described. Aryl-trienoic acid RXR agonists either unbranched[35], locked by one[36] or with multiple-fused[37] rings were reported by Boehm et al., and **5** exemplifies the latter. The substitution of a fluorine atom for a hydrogen atom adjacent to the acid group on **1** gives compound **6**[38], and substituting fluorine for the last remaining hydrogen atom adjacent to the acid group on **6** gives compound **7**[39]. Both **6** and **7** show increased RXR

activation in HCT-116 and Caco-2 cell lines, respectively. Substituting a heteroaromatic pyridine ring for the benzene ring of **1** gives compound **8**[40] and modifying the bridging alkene group of **8** to a bridging cyclopropyl group gives compound **9** (LGD100268)[40], which shows a greater potency in CV-1 cells than **1**.[40] Compound **10**[41] possesses an unsaturation in the aliphatic ring of **1**, and has been produce in kilogram quantities[42]. Acrylic acids **11**[43] (CD3254) and **12**[44] (CD2915) are also potent RXR agonists. Our group recently reported rexinoids **13** – **19**[45], as novel analogs of **8** – **11**, and several of novel **13** – **19** exhibited differential side-effect profiles and gene expression *in vivo*.[46] Recently, Kakuta and co-workers described a potent di-aryl amine carboxylic acid (**20**)[47], more commonly referred to as **NEt-TMN**[47], and several assays characterized this compound as a potent RXR agonist. Analogous compounds to **20** that have been reported include the diaryl-amine (**21**)[48] and its methylated analog (**22**)[48(a), 48(b)].

Figure 2

Kakuta and coworkers used **20** as a starting point to develop partial agonists to serve as diabetes therapeutics without the side effects profile that comes from treatment with a potent RXR agonist. However, in diseases such as cancer, there is still great need to develop additional potent RXR agonists. While weighing the side effect profiles and therapeutic potential for compounds, we must be cognizant that more effective therapeutics are often approved despite the potential for side-effects. In the case of potent RXR agonists, the more severe side-effects of hypothyroidism and triglyceridemia are often managed with hormone replacement therapy and statins. Due to the selective and potent RXR agonism observed for compounds **1** and **20**-**22**, our laboratories have recently focused on preparing the seven novel analogous compounds, **23**-**29**,

modeled after compounds **20**-**22**, as well as the sulfonic acid analogs of bexarotene, **30** and **31**. These novel rexinoids were subsequently assessed for RXR activation and EC_{50} profile, RAR cross-over, potential for causing hypertriglyceridemia, ability to inhibit cancer cell proliferation, and mutagenicity in side-by-side assays with **1** and compounds **20**-**22**.

Figure 3

Results and Discussion

Molecular Modeling

Docking scores for compounds **20**-**32** relative to bexarotene are shown in Fig. 4; each circle represents the best pose to a particular crystal structure, and $\Delta G < 0$ indicates more favorable predicted binding than bexarotene. The averaged calculated docking scores were within 1.2 kcal/mol of bexarotene, with the most favorable binding for compounds **30** and **31**. Poses of the docked compounds were largely similar to each other (this is illustrated for compounds **20** and **23** in Fig. 5), with the fused ring-systems in near identical positions and small shifts in the positions of the single rings and bridgeheads to optimize binding. The acidic groups on the single ring of the compounds were observed to hydrogen bond to Arg 315.

Figure 4 & Figure 5

The Chemistry

The route of Kakuta and co-workers was followed to reproduce **NEt-TMN** (**20**)[47(a)] from commercially available 1,1,4,4-tetramethyl-6-nitro-1,2,3,4-tetrahydronaphthalene (**32**), and details about synthetic intermediates (**33**-**36**) en route to **20** are provided (Supporting

Information). The known compound 4-(ethyl(5,5,8,8-tetramethyl-5,6,7,8-tetrahydronaphthalen-2-yl)amino)benzoic acid (**21**) was prepared using a palladium coupling method reported by Kakuta and co-workers[47(c)] , and experimental procedures for the synthetic intermediates (**37**-**39**) en route to **21** are also provided (Supporting Information). Fortuitously, compounds **20** and **21** both formed transparent, single crystals from DMSO. Hence, X-ray diffraction studies were performed and revealed the structures of **20**—incorporating DMSO within the crystal in a 1:1 ratio—and **21** (Supporting Information).

The known compound, 4-(ethyl(3,5,5,8,8-pentamethyl-5,6,7,8-tetrahydronaphthalen-2-yl)amino)benzoic acid (**22**), was synthesized in a similar method as **21**. The method of Kakuta and co-workers was used to nitrate **40** with nitric acid in acetic anhydride to give **41**[47(e)] in 50.4% yield, and **41** was subsequently reduced by palladium catalyzed reduction in a flow reactor[49] to give amine **42**[47(e)] in 97% yield. Next, amine (**42**) was coupled to **37** in a palladium (0) catalytic system to give methyl 4-((3,5,5,8,8-pentamethyl-5,6,7,8-tetrahydronaphthalen-2-yl)amino)benzoate (**43**) in 81% purified yield. Methyl ester **43** was treated with sodium hydride in DMF followed by ethyl iodide to give methyl 4-(ethyl(3,5,5,8,8-pentamethyl-5,6,7,8-tetrahydronaphthalen-2-yl)amino)benzoate (**44**) in 97% purified yield. The methyl ester of **44** was saponified under standard methanolic alkyline conditions at reflux followed by acidification with 20% hydrochloric acid to give 4-(ethyl(3,5,5,8,8-pentamethyl-5,6,7,8-tetrahydronaphthalen-2-yl)amino)benzoic acid (**22**) in 71% yield (Scheme 1). Again, a transparent crystal of **44** was given from chloroform, and an X-ray diffraction study revealed disorder in the aliphatic ring system (Supporting Information).

Scheme 1

The synthesis of novel compound 6-(ethyl(3,5,5,8,8-pentamethyl-5,6,7,8-tetrahydronaphthalen-2-yl)amino)nicotinic acid (**23**) could not be accomplished starting with an approach of coupling amine **42** to **34** through a nucleophilic aromatic substitution reaction with conditions similar to those used in the synthesis of **20**—running this type of reaction, we simply recovered **42** and **34**. Hence, we used the palladium coupling approach whereby 6-bromo-1,1,4,4,7-pentamethyl-1,2,3,4-tetrahydronaphthalene (**45**)[45] was coupled to methyl 6-aminonicotinate (**46**) to give methyl 6-((3,5,5,8,8-pentamethyl-5,6,7,8-tetrahydronaphthalen-2-yl)amino)nicotinate (**47**) in 37% purified yield. Methyl ester **47** was ethylated under standard substitution conditions to give methyl 6-(ethyl(3,5,5,8,8-pentamethyl-5,6,7,8-tetrahydronaphthalen-2-yl)amino)nicotinate (**48**) in 78% purified yield. The methyl ester of **48** was saponified in methanolic potassium hydroxide followed by acidification to give 6-(ethyl(3,5,5,8,8-pentamethyl-5,6,7,8-tetrahydronaphthalen-2-yl)amino)nicotinic acid (**23**) in 91% yield (Scheme 2).

Scheme 2

A similar route to that of Kakuta and co-workers to make **NEt-TMN**[47(a)] was followed to make novel compound 2-(ethyl(5,5,8,8-tetramethyl-5,6,7,8-tetrahydronaphthalen-2-yl)amino)pyrimidine-5-carboxylic acid (**24**). Amine (**33**) was mixed with methyl 2-chloropyrimidine (**49**) and *p*-TsOH and refluxed in 1,4-dioxane for 18 h to give methyl 2-((5,5,8,8-tetramethyl-5,6,7,8-tetrahydronaphthalen-2-yl)amino)pyrimidine-5-carboxylate (**50**) in 75% yield. Amine (**50**) in DMF was ethylated to give methyl 2-(ethyl(5,5,8,8-tetramethyl-

5,6,7,8-tetrahydronaphthalen-2-yl)amino)pyrimidine-5-carboxylate (**51**) in 75% yield. Finally, methyl ester **51** was saponified to **24** in 97% yield (Scheme 3).

Scheme 3

The novel pyrimidine compound 2-(ethyl(3,5,5,8,8-pentamethyl-5,6,7,8-tetrahydronaphthalen-2-yl)amino)pyrimidine-5-carboxylic acid (**25**), on the other hand, was prepared using the palladium coupling methodology. Aryl bromide **45** was coupled to methyl 2-aminopyrimidine-5-carboxylate (**52**) in the usual palladium (0) catalytic system to give methyl 2-((3,5,5,8,8-pentamethyl-5,6,7,8-tetrahydronaphthalen-2-yl)amino)pyrimidine-5-carboxylate (**53**) in 45% purified yield. Methyl ester **53** ethylated to give methyl 2-(ethyl(3,5,5,8,8-pentamethyl-5,6,7,8-tetrahydronaphthalen-2-yl)amino)pyrimidine-5-carboxylate (**54**) in 65% purified yield. Methyl ester **54** was saponified to give 2-(ethyl(3,5,5,8,8-pentamethyl-5,6,7,8-tetrahydronaphthalen-2-yl)amino)pyrimidine-5-carboxylic acid (**25**) in 84% yield after acidification and purification (Scheme 2).

The pyrazine analog 5-(ethyl(5,5,8,8-tetramethyl-5,6,7,8-tetrahydronaphthalen-2-yl)amino)pyrazine-2-carboxylic acid (**26**) of **NEt-TMN** was synthesized in an analogous manner using the same methodology as Kakuta.[47(a)] Amine (**33**) was reacted with methyl 5-chloropyrazine-2-carboxylate (**55**) and *p*-TsOH by refluxing in 1,4-dioxane for 18 h to give methyl 5-((5,5,8,8-tetramethyl-5,6,7,8-tetrahydronaphthalen-2-yl)amino)pyrazine-2-carboxylate (**56**) in 56 % yield. Amine (**56**) in DMF was deprotonated with sodium hydride, and the resulting anion was reacted with ethyl iodide to produce methyl 5-(ethyl(5,5,8,8-tetramethyl-

5,6,7,8-tetrahydronaphthalen-2-yl)amino)pyrazine-2-carboxylate (**57**) in 51% yield. Finally, methyl ester **57** was saponified to **26** in 71% yield under standard conditions (Scheme 3).

Again, we alternately employed the palladium coupling to access novel compound 5-(ethyl(3,5,5,8,8-pentamethyl-5,6,7,8-tetrahydronaphthalen-2-yl)amino)pyrazine-2-carboxylic acid (**27**). First, aryl-bromide **45** was coupled to methyl 5-aminopyrazine-2-carboxylate (**58**) to give methyl 5-((3,5,5,8,8-pentamethyl-5,6,7,8-tetrahydronaphthalen-2-yl)amino)pyrazine-2-carboxylate (**59**) in 63% purified yield. Methyl ester **59** was treated with sodium hydride in DMF followed by ethyl iodide to give methyl 5-(ethyl(3,5,5,8,8-pentamethyl-5,6,7,8-tetrahydronaphthalen-2-yl)amino)pyrazine-2-carboxylate (**60**) in 25% purified yield. The methyl ester of **60** was saponified under the usual conditions to provide **27** in 57% yield. (Scheme 2). Again, we were fortunate to isolate transparent crystals of **26** and **60** and X-ray diffraction studies were performed (Supporting Information).

To probe how the fluorination of **21** effects its activity, we prepared 4-(ethyl(5,5,8,8-tetramethyl-5,6,7,8-tetrahydronaphthalen-2-yl)amino)-2-fluorobenzoic acid (**28**) in a palladium coupling reaction starting from the commercially available 2-fluoro-4-iodobenzoic acid (**61**). The benzoic acid **61** was converted to methyl-ester **62** by slowly adding thionyl chloride to a solution of **61** in methanol at 0 °C followed by reflux for 1h in a modified method of Kakuta and co-workers.[47(c)] Subsequently, amine (**33**) was coupled to **62** in the standard palladium (0) catalytic system to give methyl 2-fluoro-4-((5,5,8,8-tetramethyl-5,6,7,8-tetrahydronaphthalen-2-yl)amino)benzoate (**63**) in 52% purified yield. Methyl ester **63** was ethylated to provide methyl 4-(ethyl(5,5,8,8-tetramethyl-5,6,7,8-tetrahydronaphthalen-2-yl)amino)-2-fluorobenzoate (**64**) in 68% purified yield, and **64** was saponified to make 4-(ethyl(5,5,8,8-tetramethyl-5,6,7,8-

tetrahydronaphthalen-2-yl)amino)-2-fluorobenzoic acid (**28**) in 85% yield after isolation (Scheme 1).

To complete our preparation of **NEt-TMN** analogs, novel compound 4-(ethyl(3,5,5,8,8-pentamethyl-5,6,7,8-tetrahydronaphthalen-2-yl)amino)-2-fluorobenzoic acid (**29**) was synthesized according to the route shown in Scheme 1. Amine (**42**) was coupled by palladium to 2-fluoro-4-iodo-methylbenzoate (**62**) to access methyl 2-fluoro-4-((3,5,5,8,8-pentamethyl-5,6,7,8-tetrahydronaphthalen-2-yl)amino)benzoate (**65**) in 65% purified yield. Methyl ester **65** was ethylated with ethyl iodide to methyl 4-(ethyl(3,5,5,8,8-pentamethyl-5,6,7,8-tetrahydronaphthalen-2-yl)amino)-2-fluorobenzoate (**66**) in 91% purified yield. Methyl-ester **66** was saponified to **29** in 84% yield (Scheme 1). We were pleased to recover a single crystal of **28** from DMSO, and the X-ray diffraction study structure is provided (Supporting Information).

Because of the excellent predicted binding for the sulphonic acid analog (**30**) of bexarotene (**1**), we also set out to synthesize 4-(1-(3,5,5,8,8-pentamethyl-5,6,7,8-tetrahydronaphthalen-2-yl)vinyl)benzenesulfonic acid (**30**) and its ketone analog 4-(3,5,5,8,8-pentamethyl-5,6,7,8-tetrahydronaphthalene-2-carbonyl)benzenesulfonic acid (**31**). Commercially available potassium 4-carboxybenzenesulfonate (**67**) was refluxed in thionyl chloride and thereby converted to 4-(chlorosulfonyl)benzoyl chloride (**68**). Benzoyl chloride (**68**) was mixed with **40**, and when aluminum chloride was added to the mixture, the Friedel-Crafts acylation provided 4-(3,5,5,8,8-pentamethyl-5,6,7,8-tetrahydronaphthalene-2-carbonyl)benzene-1-sulfonyl chloride (**69**) in 86% yield. Sulfonyl chloride **69** was converted to **31** in 56% yield by treatment of **69** with sodium hydroxide in acetone followed by acidification with 20% HCl. Sulfonyl chloride **69** was also observed to react with 2-methylpropanol in acetone and triethylamine to give isobutyl 4-(3,5,5,8,8-pentamethyl-5,6,7,8-

tetrahydronaphthalene-2-carbonyl)benzenesulfonate (**70**) in 87% yield. When the isobutyl sulfonate ester **70** was treated with a solution of triphenylphosphine methylide, isobutyl 4-(1-(3,5,5,8,8-pentamethyl-5,6,7,8-tetrahydronaphthalen-2-yl)vinyl)benzenesulfonate (**71**) was produced in 48.9% yield. The vinyl sulfonate (**71**) was refluxed with KOH in methanol and then treated with 20% HCl to give 4-(1-(3,5,5,8,8-pentamethyl-5,6,7,8-tetrahydronaphthalen-2-yl)vinyl)benzenesulfonic acid (**72**) in 80% yield (Scheme 4).

Scheme 4

Biological Assays and Rationale

Mammalian two-hybrid assay demonstrates that several novel analogs induce RXR homodimerization: Biologic evaluation of the synthetic analogs described above (compounds **20-31**) was first conducted using the mammalian two-hybrid system in the human colorectal carcinoma cell line, HCT116. Employing this assay, ligand binding to a recombinant RXR containing an activation domain will induce dimerization with an RXR-Gal4 fusion protein. The subsequent dimer will then bind to multiple Gal4 DNA response elements which are used to drive expression of firefly luciferase.

We tested the indicated compounds at three different concentrations (25 nM, 100 nM and 1000 nM) in this system. The 25 nM assay revealed that five compounds (**20, 23, 24, 25, 29, 22**) possessed transcriptional activity considerably higher than compound **1** (bexarotene). Compounds **20, 23, 24** and **25** revealed transcriptional activity that was 2-fold higher than compound **1**, while compound **29** and **22** was increased 40-50% (Figure 6A). Conversely,

compounds **31, 30, 27** and **26** were dramatically reduced in their ability to induce RXR homodimerization and displayed activity of 0.6, 0.8, 3.4 and 11.3% when compared to compound **1**, respectively. At 100 nM treatment (Figure 6B), four compounds (**20, 23, 24** and **25**) exhibited increased transcriptional activity in the range of 135-146%, when compared to compound **1**. Additionally, compounds **29, 22, 28, 21** had activity similar to compound **1.** Analogous to the 25 nM treatment (Figure 6A), compounds **31** and **30** were not able to induce RXR homodimerization, but analogs **26** and **27** exhibited a significant increase in activity (5 to 16-fold) at the higher 100 nM analog concentration (compare Figure 6A and 6B). Furthermore, at 1000 nM treatment (Figure 6C), compounds **20, 23, 24, 25** and **26** exhibited activities greater than compound **1**, with activity increased by 35-58%. In contrast, even at this elevated concentration, compound **31** was not able to induce RXR homodimerization, while compound **30** had activity of 17% compared to compound **1**. Interestingly, compounds **29** and **22** exhibited the greatest transcriptional activity at 25 nM (140% and 150% of compound **1**) and lower activity at 1000 nM (51-56% of compound **1)**. These results indicate that novel analogs modeled after compound **1** can be generated that increase RXR homodimerization, presumably via increased binding to RXR (see Table 1). Furthermore, acidification of the molecule does not increase RXR homodimerization, as illustrated with compounds **31** and **30.** Also, fluorination does not alter homodimerization, as shown by testing of compounds **29** and **28** compared to **22** and **21**.

Figure 6

Determination of EC_{50} values: We utilized the mammalian two-hybrid system in HCT116 colon cancer cells to determine the EC_{50} value for compounds **20-31**. Full dose response curves were

generated using a wide range of analog concentrations of 0.1 nM to 2000 nM for compounds **20-29** and 1 μM to 80 μM for compounds **31** and **30**. The results reveal that compounds **20, 23, 24, 25, 29,** and **22** have an EC_{50} lower than compound **1,** with EC_{50} values of 13.8, 13.8, 40.9, 18.2, 33.8 and 7.9 nM, respectively (Table 1). These results are not surprising because these compounds exhibited greater RXR homodimerization at 25 nM compared to compound **1** (Figure 7A). In contrast, compounds **26, 27, 28** and **21** have EC_{50} values that were 2.4 to 7-fold higher than compound **1**. As observed in the mammalian two-hybrid assay (Figure 6), acidification of the parent compound **1** to generate **30** and **31** resulted in decreased homodimerization, and the EC_{50} for compound **30** was determined to be approximately 18,200 nM which is 350-fold higher than compound **1**, while an EC_{50} value for **31** could not be calculated even when dosing at 80,000 nM.

The EC50s for **30** and **31** were surprising, since docking predicted highly favorable binding (Fig. 1), with hydrogen bonding between the sulfonate of the compounds and Arg 315 of the RXR (residue numbering as in 1MVC[50]). This disagreement could stem from the implicit solvent, which might mistreat dehydration.[51] Alternatively, compounds **30** and **31** may bind to RXR but not activate the receptor, a profile that would be more indicative of an antagonist. Therefore, we conducted competitive binding experiments in which we treated HCT-116 cells with increasing concentrations of **30** and **31** and a standard concentration of bexarotene, and these experiments revealed decreasing bexarotene-directed activation of RXR in the presence of increasing **30** and **31** (Figure S12 in the Supporting Information). These results suggest that **30** and **31** likely reach the binding pocket of RXR, but they appear to exert antagonism compared to **1**. Finally, it is interesting to note that compounds **20** and **23** exhibit almost identical EC_{50} values

(Table 1), and the best docked poses (Fig. 4) suggest very similar modes of binding despite the structural difference of a methyl substitution.

Table 1

Novel analogs are able to direct RXR/RXRE homodimer-mediated transcription: The mammalian two-hybrid assay is a useful, initial screen for RXR agonist induced homodimerization because of its accessibility, speed and sensitivity. However, it is necessary to determine if RXR agonists are able to induce transcription in a natural protein and DNA configuration. Therefore, we performed a second screening assay that utilizes transfection of human RXRα and an authentic RXRE from the rat cellular retinol binding protein II gene. As with the mammalian two-hybrid assay, three concentrations of compounds were used, 25 nM, 100 nM and 1000 nM. At 25 nM (Figure 7A) compounds **20, 23, 24, 25, 29**, **22** and **28** exhibited increased RXR-mediated transcriptional activity when compared to compound **1**, with the values being amplified by 27-66%. The greatest activity was observed with compounds **20, 23, 24**, and **25**. These results are similar to those obtained in the mammalian two-hybrid system (Figure 6A). Taken together, it is suggested that at 25nM compounds **20, 23, 24, 25, 29**, **22** and **28** are more efficient than compound **1** at binding to RXR and inducing RXR homodimerization, DNA binding and initiation of transcription via an RXRE. Conversely, compounds **31, 30, 26** and **27** are not as effective at initiating transcription from an RXRE as compound **1**. As expected from the mammalian two-hybrid assay, compound **31** was unable to initiate transcription above the solvent control. At 100 nM, compounds **20, 23, 24** and **25** exhibited a 68-89% increase in transcriptional activity when compared to compound **1** (Figure 7B). Compounds **29, 22, 28,** and **21** showed slight increases in RXRE transcription of approximately 16-32%. At 1000 nM, only

compounds **20, 23, 24, 25** and **26** exhibited increased activity, ranging from 20-43% (Figure 7C). Interestingly, compounds **27, 29, 22, 28** and **21** displayed similar RXRE activity as compound **1**, despite having reduced activity in the mammalian two-hybrid system (compare Figure 6C and 7C), suggesting that the specific DNA platform recognized by the RXR homodimer may play a role in agonist-receptor affinity/activity.

Figure 7

Quantitation of RAR agonist activity: Since compound **1** is known to possess "residual" retinoic acid receptor (RAR) agonist activity, we evaluated the ability of compounds **20-31** to induce transcription via the retinoic acid response element (RARE) and RAR. Human embryonic kidney cells (HEK293) cells were transfected with human RARα and dosed with 100 nM of either all-*trans* retinoic acid (RA), the natural ligand for RARα, compound **1** or analogs. Within this assay, compound **1** possessed 27% of the activity of RA (Figure 8A). Compound **20** displayed the greatest RARE activation at 26% of RA, while compound **29** showed the lowest RARE activity at 11%, which is indistinguishable from the ethanol control. Since one goal of this work was to develop specific RXR agonists, an index of cross-reactivity (CR) was generated by calculating the RARE:RXRE ratio, with compound **1** set to 1.0. Figure 8B reveals that RA, as expected, has a very high index of cross-reactivity with a ratio of 9.5 indicating a preference to activate RAR over RXR. Conversely, compounds **25, 29, 22** and **28** have the lowest cross-reactivity index at 0.35-0.37, indicating that they preferentially bind and activate RXR 3-fold more efficiently than RAR (compared to the parent compound **1**). Compounds **20, 26** and **27**

have a CR>0.5. Taken together, this assay reveals that compounds **20-29** have a lower CR than compound **1** suggesting that they are more selective RXR agonists than the parent compound.

Figure 8

Evaluation of SREBP promoter activation: One of the primary side effects of treatment with bexarotene (compound **1**) is hypertriglyceridemia. Lipid metabolism is regulated, in part, by the sterol regulatory element-binding proteins (SREBPs), which are a group of transcription factors that regulate genes involved in lipid biosynthesis. Expression of SREBP is regulated in part by the liver X receptor (LXR)/RXR heterodimer via LXRE control elements in the SREBP promoter. We tested the ability of compounds **20-31** to activate the SREBP promoter alone or in the presence of the LXR agonist TO901317 (TO). Figure 9A shows that compounds **26, 27, 29, 22, 28** and **21** have decreased transcriptional activity, ranging from 54-79% of the activity of compound **1**, while compounds **20, 23, 24** and **25** have a similar activity profile relative to compound **1.** Not surprisingly, compounds **31** and **30**, which do not activate RXR (Figures 6 and 7), do not stimulate the SREBP promoter and the activity of these analogs is similar to the ethanol control. Furthermore, in the presence of analog and TO (activated LXR), only compounds **26, 27, 28** and **21** show reduced SREBP promoter activation, compared to compound **1** and TO. Compound **26** + TO shows a reduction of 33% and compound **27** displays a 29% reduction. Although compounds **20, 23, 24** and **25** have similar transcriptional activity as compound **1**, alone, there is a 13-17% decrease when combined with TO. The lipid risk assessment (LR) was generated by calculating the SREBP:RXRE activity ratio and is a measure of the potential risk of SREBP-driven hypertriglyceridemia associated with patient treatment of

compound **1**. Compounds **26, 29, 22** and **28** show a LR ranging from 0.48-0.65 (Figure 9B), with compounds **29, 22, 28** and **21** possessing both an *increase* in RXRE transcriptional activity (Figure 7B) and a *decrease* in SREBP transcription (Figure 9A), when compared to compound **1**. These results suggest that it is possible to generate analogs of compound **1** with increased RXR activity, while potentially decreasing adverse side effects of hypertriglyceridemia. Conversely, compound **27** possesses both a decrease in RXR/RXRE transcriptional assays (Figure 7B) and a decrease in SREBP promoter activity (Figure 9A). Furthermore, the LR for compounds **20, 23, 24** and **25** range from 0.49-0.51 as a result of increased transcriptional activity in the RXRE assay of 68-89% (Figure 7B), while maintaining similar SREBP transcriptional activity as compound **1** (Figure 9A). In summary, the results for compounds **20, 23, 24**, **25** and **28** indicate that these compounds display at least a 2-fold preference for activating RXR/RXRE transcription versus SREBP (i.e., an LR of ≤ 0.50).

Figure 9

Evaluation of RXR-mediated induction of CYP3A4: CYP3A4 is a member of the cytochrome P450 family of proteins and is responsible for the oxidation and clearance of approximately 50% of xenobiotics by the liver. It has been shown that compound **1** is sufficient to induce CYP3A4 expression.[52] We tested compounds **20-31** for their ability to induce CYP3A4 mRNA expression using qPCR in the liver carcinoma cell line HepG2. There was variable induction of CYP3A4 ranging from a 3-fold repression (compound **28)**, to a 2-fold induction for compounds **31** and **24**, while compound **1** resulted in a 3.2-fold induction (Figure 10). In addition to compound **28**, compound **21** also repressed CYP3A4 expression by 2.3-fold. Compounds **23** and **29** did not

alter CYP3A4 expression, while compounds **20, 25, 26** and **27** resulted in a modest increase of approximately 1.5-fold in CYP3A4 expression. These results demonstrate that for one metabolic breakdown pathway, compounds **20-31** exert repressive effects that *in vivo* (depending on the totality of metabolism that occurs) could potentially translate into differential half-life profiles for these compounds compared to **1**, as previously observed by our group.[46]

Figure 10

Inhibition of proliferation in CTCL cells: Since compound **1** is used clinically to treat cutaneous T-cell lymphoma (CTCL), compounds **20-31** were evaluated for their ability to inhibit growth of the CTCL cell line, Hut78. Figure 11 indicates that none of the compounds tested were as efficient at inhibiting Hut78 growth as compound **1**. However, compounds **20, 23** and **24** were able to inhibit growth >85% as efficiently as compound **1**. Furthermore, compounds **25, 29** and **21** also maintained 55-80% of the anti-proliferative capacity of the parent compound **1**. There was a substantial decrease in the anti-proliferative effects of compounds **26, 27, 22** and **28**, which were only 35-51% as effective as compound **1**.

Figure 11

Inhibition of HDAC1 expression in CTCL cells: Since none of the novel analogs tested were as effective at inhibiting cell growth of Hut78 cells, we examined the ability of a subset of analogs, **20** and **25** to inhibit histone deacetylase-1 (HDAC1) expression. HDAC inhibitors have been in development for several years with four receiving FDA approval, including Vorinostat for

treatment of CTCL.[53] Figure 12 shows that compound **1** was able to suppress HDAC1 expression by 10%, while compound **25** showed a 28% reduction. Surprisingly, compound **20** did not alter HDAC1 expression. These data suggest, that although compound **25** did not inhibit growth as effectively as compound **1** in the proliferation assay (Figure 11), it may be more effective at inducing toxicity or apoptosis by altering gene expression and protein function, compared to compound **1**.

Figure 12

Mutagenesis: Further determining the suitability of the compounds, we undertook a screen of the compounds to test for their ability to mutate DNA, a very undesirable trait in any potential pharmaceutical. We assayed the compounds as in previous work[39, 45] and determined that none of the compounds are mutagenic in this assay.

Conclusions

Bexarotene (**1**) possesses FDA approval for cutaneous T-cell lymphoma, and has been examined in a plethora of other cancer types. Recent studies also suggest that **1** may be a promising candidate to treat Alzheimer's disease (AD).[29, 54] The current study was interested in factors that may mitigate the side-effect profile of **1**, since bexarotene appears to effectively treat many CTCL patients, but also has the potential to activate RXR heterodimer pathways and thereby induce hyperlipidemia and hypothyroidism. There is compelling motivation to explore novel RXR ligands for therapeutic treatment, since new rexinoids may possess unique activities and reduced side-effect profiles, and we have previously demonstrated[39, 45] a number of novel

rexinoids with different PK characteristics and differential ability to modulate RXR-controlled pathways.[46] The current study has produced 9 rexinoids, 5 of which were determined to possess lower EC_{50}s than **1**. More potent rexinoids, possessing lower EC_{50} values, may be able to translate to clinical treatments permitting lower dose regimens to achieve the same effect in patients, and this may have the potential to reduce dose-dependent side-effects. We address the primary concern about rexinoids' tendency to raise lipids by assessing this panel of analogs in an SREBP assay. Interestingly, compounds **21, 22, 28** and **29** all exhibit greater RXRE activation and reduced SREBP promotion versus **1**. Furthermore, given the recent development of vorinostat and romidepsin histone deacetylase inhibitors (HDACi), and FDA approved of these HDACi for the treatment of cutaneous T-cell lymphoma (CTCL), we found that compound **25** exhibited a greater suppression of HDAC1 than **1**. Moreover, several of the rexinoids **20**-**31** also demonstrated similar anti-proliferative effects in Hut78 cells as well as a lower induction of CYP3A4 as **1**—suggesting that some of the novel rexinoids may perhaps possess modified half-life profiles in comparison to **1**. Taken together, a number of our novel RXR agonists in this study exhibit greater on-target potency, similar efficacy at inhibition of CTCL proliferation, and a lower likelihood to induce side effects than **1**.

Experimental Section

Ligand Docking and Scoring. Docking studies were carried out for bexarotene and ligands **20**-**31**. The ligands were prepared by Avogadro[55], following an energy minimization with the Universal Force Field[56]. The charge distribution on ligands were assigned by Autodock[57] and OpenBabel 2.3.0[58], respectively. Prepared ligands were docked to a group of target proteins, which include the human RXRα (protein data bank code 1MVC[50], 1MZN[50], 1RDT[59], 2P1T[8],

2P1U[8], 2ZXZ[60], 2ZY0[60], 3DZY[61], 3DZU[61], 3E00[61], 3FUG[43], 3H0A[62], 3PCU[63], 4K6I[62], respectively) and RXRβ (protein data bank code 1H9U[64]). Docking was performed using the Autodock 4.2 software[57]. As in our previous studies[39, 45], protein residues Arg 316 and Ile 268 (residue numbering as in 1MVC) were treated flexible. Docking used the Lamarckian genetic algorithm with 25,000,000 energy evaluations per dock and a total of 250 docks per compound. Calculated binding free energies were used to score the compounds.

Mammalian Two-Hybrid Assay. HCT-116 colorectal carcinoma cells were plated overnight at 80,000 cells per well in a 24-well plate and maintained in DMEM + glutamine + sodium pyruvate (Mediatech, Manassas, VA) containing 10% FBS (Atlanta Biologicals, Atlanta, GA), supplemented with 100 μg/mL streptomycin and 100 U/mL penicillin. (Gibco, Gaithersberg, MD). Cells were co-transfected using a human RXR binding domain (BD) vector (bait), a human RXR activation domain (AD) vector (prey), pFR-Luc and renilla control plasmid. Transfection was conducted using 1.25 μL of Polyjet (Signagen, Gaithersberg, MD) per well and allowed to incubate for 24 hours. The cells were then treated with ethanol or DMSO vehicle (0.1%), compound 1 or the indicated analogs at a final concentrations of 25 nM, 100 nM or 1000 nM and incubated for 24 hours. The rexinoid activity was measured by luciferase output utilizing a dual-luciferase report assay system according to the manufacturer's instructions (Promega, Madison, WI) in a Sirus luminometer (Berthold Detection System, Pforzheim, Germany). Three independent assays were conducted with triplicate samples for each treatment group. The value of compound 1 is set to 100%.

EC_{50} Determination. The EC_{50} values were determined from full dose-response curves for compound **1** and compounds **20**-**29** ranging from 0.1 to 2000 nM. EC_{50} curves for **30** and **31** were determined from dose-response curves ranging from 1 to 80 μM. HCT-116 cells were

plated, transfected and treated as above using the mammalian two-hybrid assay protocols. Cells were treated with ethanol or DMSO vehicle (0.1%) or analog (final concentration of 0.1, 0.5, 1, 2.5, 5, 10, 25, 50, 75, 100, 250, 500, 750, 1000, 2000 nM) for 24 hours. Alternatively, compound **30** and **31** dose curves were generated using a final concentration of 1, 2.5, 5, 10, 20, 40, 80 μM. The amount of rexinoid activity at each concentration was measured using the same luciferase assay described above. Dose response curves were generated using 4-parameter analysis utilizing Prism Software (GraphPad Inc., La Jolla, CA). Three independent assays were conducted with triplicate samples for each treatment group.

RXRE-mediated Transcription Assay. HCT-116 cells were plated at 80,000 cells per well in a 24-well plate and maintained as described above. The cells were co-transfected using 250 ng of RXRE-luciferase reporter gene (RXRE from the naturally occurring responsive element in rat cellular retinol binding protein II gene: 5'-AAAATGAACTGTGACCTGTGACCTGTGACCTGTGAC-3', DR1 responsive elements underlined), 25 ng pSG5-human RXRα and 20 ng of renilla control plasmid using 1.25 μL Polyjet for 24 hours. The cells were treated with ethanol or DMSO vehicle (0.1%) or analog (final concentration of 25 nM, 100 nM or 1000 nM) for 24 hours. The rexinoid activity was measured by luciferase output as described above. Three independent assays were conducted with triplicate samples for each treatment group. The value of compound 1 is set to 100%.

RARE-mediated Transcription Assay. HEK293, human embryonic kidney, cells were plated at 60,000 cells per well in a 24-well plate and maintained as described above. After 24 hours, the cells were transfected with 250 ng pTK-DR5(X2)-Luc, 25 ng pCMX-human RARα and 20 ng renilla utilizing 1.25 μL Polyjet per well for 24 hours. The sequence of the double DR5 RARE is: 5'-AAAGGTCACCGAAAGGTCACCATCCCGGGAGGTCACCGAAAGGTCACC-3'

(DR5 responsive elements underlined). The cells were treated with ethanol or DMSO vehicle (0.1%) or all-*trans*-retinoic acid (RA, the ligand for RAR) or the indicated rexinoid at a final concentration of 100 nM. After 24 hours of treatment, the retinoid activity was measured as described above. The activity of compound 1 or analog divided by the activity of all-*trans*-RA (expressed as a percentage) represents the RAR agonist activity. Three independent assays were conducted with triplicate samples for each treatment group. The value for RA is set to 100%. The "index of cross-reactivity" was calculated by dividing RARE activity by 100 nM RXRE activity with the RARE:RXRE ratio for compound 1 set to 1.0.

Sterol Regulatory Element-Binding Protein (SREBP)-mediated Transcription Assay. HCT116 colorectal carcinoma cells were plated at 80,000 cells per well and maintained as described above. After 24 hours, the cells were co-transfected with 100 ng pBP1c(6500)-Luc which contains approximately 6500 base pairs of the flanking DNA from the murine sterol regulatory element binding protein (SREBP)-1c natural promoter, along with 10 ng pCMX-hLXRα and 20 ng of renilla control plasmid using 1.25 μL Polyjet for 24 hours. The cells were treated with 100 nM of the LXR agonist TO901317 alone or with 100 nM compound 1 or analog. After 24 hours, the amount of SREBP promoter activity was measured by luciferase output as described above. Three independent assays were conducted with triplicate samples for each treatment group. The value of compound **1** is set to 100%. The "lipid risk assessment" was calculated by dividing SREBP activity by 100 nM RXRE with the SREBP:RXRE ratio for compound **1** set to 1.0.

Proliferation Assay. Human T-cell lymphoma cells (Hut78) were maintained in RPMI media (Mediatech, Manassas, VA) containing 10% FBS (Atlanta Biologicals, Atlanta, GA), supplemented with 100 μg/mL streptomycin and 100 U/mL penicillin (Gibco, Gaithersberg,

MD) at 37°C, 5% CO_2. Cells were plated at 7,500 cells per well in a 96-well plate and immediately dosed with either media alone, ethanol, DMSO or 200 nM of compound 1 or analog in a total volume of 100 µL. After 72 hours, 20 µL of CellTiter 96 AQ_{ueous} One Solution Cell Proliferation Assay (MTS) (Promega, Madison, WI) was added to each well and the plate was incubated at 37°C according to manufacturer's recommendations. MTS assays were quantified using a BioTek ELx808 96-well plate reader (BioTek, Winooski, VT) at A_{490} nm. Percent inhibition was calculated using media control set to 0.0.

Quantitative real-time PCR. Human hepatocellular carcinoma cells (HepG2) cells were maintained in DMEM + glutamine + sodium pyruvate (Mediatech, Manassas, VA) containing 10% FBS (Atlanta Biologicals, Atlanta, GA), supplemented with 100 µg/mL streptomycin and 100 U/mL penicillin (Gibco, Gaithersberg, MD). Cells were plated at 400,000 cells per well in a 6-well plate. After 16 hours, the media was replaced with DMEM containing 1% FBS for 24 hours. The cells were dosed in DMEM-1% FBS containing ethanol, DMSO or compound 1 or analog for 24 hours. Total RNA was isolated from each plate or well using an Aurum Total RNA Mini kit (Bio-Rad, Hercules, CA) according to the manufacturer's instructions. The RNA obtained was quantified using A260/280 spectrophotometry.

Human T-cell lymphoma cells (Hut78) were maintained in RPMI media as described above. Cells were harvested by centrifugation, 10 minutes at 400 rcf at room temperature, and resuspended in RPMI supplemented with 1% FBS, 100 µg/mL streptomycin and 100 U/mL penicillin. Cells were plated at 750,000 cells per well in a 6-well plate and immediately dosed with ethanol, DMSO, compound or analog at a final concentration of 100 nM for 48 hours. Total RNA was extracted as described above.

DNase-treated total RNA (0.5 μg) was reverse-transcribed via the use of the iScript cDNA Synthesis kit (Bio-Rad) to prepare 20 μL of first strand cDNA. Real-time PCR reactions were prepared by adding 1.5 μL of cDNA to 5 μL FastStart Universal SYBR Green Master Mix + Rox (Roche Applied Science, Indianapolis IN) and primers for a total volume of 10 μL. Reactions were performed in 96 well plates in a BioRad CFX96 thermal cycler using a 40 cycle profile. Data analysis was performed using the comparative ΔΔCt method as the means of relative quantitation, normalized to an endogenous reference (GAPDH) and relative to a calibrator (normalized Ct value from vehicle-treated cells) and expressed as $2^{-\Delta\Delta Ct}$ according to Applied Biosystems' User Bulletin 2: Rev B, "Relative Quantitation of Gene Expression." The primers utilized during PCR experimentation are as follows: GAPDH forward: 5'-ACAACTTTGGTATCGTGAAGGAC-3', GAPDH reverse: 5'-CAGGGATGATGTTCTGGAGAGC-3'; HDAC1 forward: 5'-GAGATGACCAAGTACCACAGC-3' HDAC1 reverse: 5'-TGACAGAACTCAAACAGGCC-3'; CYP3A4 forward: 5'-TCAGCCTGGTGCTCCTCTATCTAT -3' CYP3A4 reverse: 5'-AAGCCCTTATGGTAGGACAAAATATTT -3'.

Mutagenesis Assay. All compounds were tested for their ability to mutate DNA in an EPA-approved *Saccharomyces cerevisiae* cell based system as in our previous work.[39, 45] D7 yeast cells[65] were incubated with increasing concentrations of each compound solubilized in DMSO (highest concentration being 0.1mg/ml) and then plated on yeast extract, peptone, dextrose media; and synthetic media lacking isoleucine or tryptophan, to check for forward and reverse mutations.[66]

Instrumentation. A 400 MHz Bruker spectrometer was used to acquire ^{1}H NMR and ^{13}C NMR spectra. Chemical shifts (δ) are listed in ppm against residual non-deuterated solvent peaks in a

given deuterated solvent (e.g. $CHCl_3$ in $CDCl_3$) as an internal reference. Coupling constants (*J*) are reported in Hz, and the abbreviations for splitting include: s, single; d, doublet; t, triplet; q, quartet; p, pentet; m, multiplet; br, broad. All ^{13}C NMR spectra were acquired on a Bruker instrument at 100.6 MHz. Chemical shifts (δ) are listed in ppm against deuterated solvent carbon peaks as an internal reference. High resolution mass spectra were recorded using either a JEOL GCmate(2004), a JEOL LCmate(2002) high resolution mass spectrometer or an ABI Mariner (1999) ESI-TOF mass spectrometer.

General Procedures. Removal of volatile solvents transpired under reduced pressure using a Büchi rotary evaporator and is referred to as removing solvents *in vacuo*. Thin layer chromatography was conducted on precoated (0.25 mm thickness) silica gel plates with 60F-254 indicator (Merck). Column chromatography was conducted using 230-400 mesh silica gel (E. Merck reagent silica gel 60). All tested compounds were analyzed for purity by combustion analysis through Columbia Analytical Services (formerly Desert Analytics in Tucson, AZ) and were found to be > 95% pure.

NEt-TMN (20).[47(a)] To a 100 mL round-bottomed flask equipped with a stir bar and charged with 6-(ethyl(5,5,8,8-tetramethyl-5,6,7,8-tetrahydronaphthalen-2-yl)amino)nicotinate (0.3674 g, 1.002 mmol) suspended in methanol (3.5 mL) was added a solution of potassium hydroxide (0.1767 g, 3.15 mmol) in water (0.22 mL). This reaction was stirred at reflux in an oil bath at 87 °C for 1 h. The reaction was then cooled to room temperature and acidified with 20% HCl (52 mL). The crude white precipitate was filtered and washed with cold water to provide crude **20** (0.3238 g, 91%) and this crude material was purified by column chromatography (25 mL SiO_2,

30% ethyl acetate:hexanes to pure ethyl acetate to 2% methanol:ethyl acetate) to give **20** (0.2677 g, 76%) as a white crystalline solid, m.p. 230-232 °C (lit. 235.7 – 237.7 °C): ^{1}H NMR (400 MHz, d6-DMSO) δ 12.44 (br s, 1H), 8.66 (dd, *J* = 2.4, 0.4, 1H), 7.78 (dd, *J* = 8.8, 2.4, 1H), 7.43 (d, *J* = 8.0, 1H), 7.18 (d, *J* = 2.0, 1H), 7.01 (dd, *J* = 8.4, 2.4, 1H), 6.19 (dd, *J* = 9.2, 0.4, 1H), 3.94 (q, *J* = 6.8, 2H), 1.66 (s, 4H), 1.26 (s, 6H), 1.22 (s, 6H), 1.22 (t, *J* = 6.8, 3H); ^{13}C NMR (100.6 MHz, d6-DMSO) δ 166.6, 159.7, 150.5, 146.5, 143.1, 140.7, 137.6, 128.1, 125.4, 124.8, 114.7, 106.7, 44.7, 34.5. 34.4, 34.0, 33.8, 31.5, 31.4, 12.7; IR (neat) 2925, 1666, 1592, 1409, 1274 cm^{-1}; ES-MS (M-H)- calcd for $C_{22}H_{27}N_2O_2$ 351.2072, found 351.2073. Anal. Calcd for $C_{22}H_{28}N_2O_2$: C, 74.97; H, 8.01; N, 7.95. Found: C, 74.74; H, 8.38; N, 7.56.

4-(Ethyl(5,5,8,8-tetramethyl-5,6,7,8-tetrahydronaphthalen-2-yl)amino)benzoic acid (21). Compound **21** was synthesized following the same general procedure to make **20** to give pure **21** as a white crystalline solid, m.p. 247.8-250.6 °C: ^{1}H NMR (400 MHz, d6-DMSO) δ 12.14 (br s, 1H), 7.69 (d, *J* = 9.2, 2H), 7.38 (d, *J* = 8.4, 1H), 7.12 (d, *J* = 2.0, 1H), 6.95 (dd, *J* = 8.4, 2.4, 1H), 6.64 (d, *J* = 8.8, 2H), 3.72 (q, *J* = 7.2, 1H), 1.65 (s, 4H), 1.26, (s, 6H), 1.21 (s, 6H), 1.13 (t, *J* = 7.2, 3H); ^{13}C NMR (100.6 MHz, d6-DMSO) δ 167.2, 151.1, 146.1, 142.6, 141.9, 130.9, 127.9, 124.6, 124.1, 118.2, 112.6, 34.5, 34.4, 34.0, 33.7, 31.5, 31.4, 12.1; IR (neat) 2955, 1661, 1594, 1270, 1180 cm^{-1}; ES-MS (M-H)- calcd for $C_{23}H_{28}NO_2$ 350.2120, found 350.2122. Anal. Calcd for $C_{23}H_{29}NO_2$: C, 78.59; H, 8.32; N, 3.99. Found: C, 78.30; H, 8.70; N, 3.87.

4-(Ethyl(3,5,5,8,8-pentamethyl-5,6,7,8-tetrahydronaphthalen-2-yl)amino)benzoic acid (22). Compound **22** was synthesized following the same general procedure to make **20** to give pure **22** as a white crystalline solid, m.p. 252.4-256.8 °C: ^{1}H NMR (400 MHz, d6-DMSO) δ 12.06 (br s,

1H), 7.68 (d, *J* = 9.2, 2H), 7.28 (s, 1H), 7.02 (s, 1H), 6.40 (d, *J* = 8.8, 2H), 3.62 (br s, 2H), 1.97 (s, 3H), 1.63 (s, 4H), 1.25, (s, 6H), 1.19 (s, 6H), 1.14 (t, *J* = 7.2, 3H); ^{13}C NMR (100.6 MHz, d6-DMSO) δ 167.3, 151.1, 144.0, 143.2, 140.7, 132.8, 131.1, 129.1, 126.6, 117.3, 110.7, 45.4, 34.6, 34.4, 33.7, 33.6, 31.6, 31.5, 17.0, 12.2; IR (neat) 2957, 1665, 1597, 1274, 1176 cm^{-1}; ES-MS (M-H)- calcd for $C_{24}H_{30}NO_2$ 364.2277, found 364.2268. Anal. Calcd for $C_{24}H_{31}NO_2$: C, 78.86; H, 8.55; N, 3.83. Found: C, 78.87; H, 8.91; N, 3.76.

6-(Ethyl(3,5,5,8,8-pentamethyl-5,6,7,8-tetrahydronaphthalen-2-yl)amino)nicotinic acid (23). The same methodology to synthesize **20** gave pure **23** as a white crystalline solid, m.p. 250.2-251.0 °C: ^{1}H NMR (400 MHz, d6-DMSO) δ 12.42 (br s, 1H), 8.66 (d, *J* = 2.0, 1H), 7.78 (dd, *J* = 8.8, 2.0, 1H), 7.32 (s, 1H), 7.07 (s, 1H), 5.89 (br s, 1H), 4.19-4.05 (m, 1H), 3.65-3.55 (m, 1H), 1.98 (s, 3H), 1.64 (s, 4H), 1.26 (d, *J* = 6.4, 6H), 1.20 (s, 6H), 1.13 (t, *J* = 7.2, 3H); ^{13}C NMR (100.6 MHz, d6-DMSO) δ 166.6, 159.5, 150.7, 144.1, 143.8, 139.0, 137.9, 132.5, 129.2, 126.5, 114.4, 105.9, 44.0, 34.5, 34.4, 33.7, 31.6, 31.5, 16.9, 12.7; IR (neat) 2960, 1669, 1595, 1509, 1412, 1266 cm^{-1}; ES-MS (M-H)- calcd for $C_{23}H_{29}N_2O_2$ 365.2229, found 365.2235. Anal. Calcd for $C_{23}H_{30}N_2O_2$: C, 75.37; H, 8.25; N, 7.64. Found: C, 75.33; H, 8.46; N, 7.56.

2-(ethyl(5,5,8,8-tetramethyl-5,6,7,8-tetrahydronaphthalen-2-yl)amino)pyrimidine-5-carboxylic acid (24). The same methodology to synthesize **20** gave **24** (0.3668 g, 97%) as a white crystalline solid, m.p. 249.5-250.6 °C: ^{1}H NMR (400 MHz, d6-DMSO) δ 12.62 (br s, 1H), 8.37 (s, 1H), 7.35 (d, *J* = 8.4, 1H), 7.17 (d, *J* = 2.4, 1H), 7.00 (dd, *J* = 8.4, 2.0, 1H), 3.99 (q, *J* = 7.2, 2H), 1.67 (s, 4H), 1.27 (s, 6H), 1.24 (s, 6H), 1.16 (t, *J* = 7.2, 3H); ^{13}C NMR (100.6 MHz, d6-DMSO) δ 165.1, 161.9, 159.1, 15.2, 142.3, 140.2, 126.8, 124.7, 124.6, 113.5, 45.3, 34.4, 34.4,

33.7, 33.5, 31.4, 31.3, 12.3; IR (neat) 2962, 1664, 1586, 1515, 1426, 1278 cm^{-1}; ES-MS (M-H)- calcd for $C_{21}H_{26}N_3O_2$ 352.2025, found 352.2024. Anal. Calcd for $C_{21}H_{27}N_3O_2$: C, 71.36; H, 7.70; N, 11.89. Found: C, 71.40; H, 7.98; N, 11.79.

2-(Ethyl(3,5,5,8,8-pentamethyl-5,6,7,8-tetrahydronaphthalen-2-yl)amino)pyrimidine-5-carboxylic acid (25). The same methodology to synthesize **20** gave pure **25** as a white crystalline solid, m.p. 231.9-233.1 °C: ^{1}H NMR (400 MHz, d6-DMSO) δ 12.60 (br s, 1H), 8.74 (br s, 2H), 7.23 (s, 1H), 7.05 (s, 1H), 4.04 (sextet, *J* = 7.2, 1H), 3.76 (sextet, *J* = 7.2, 1H), 1.97 (s, 3H), 1.65 (s, 4H), 1.29, (s, 3H), 1.26 (s, 3H), 1.23 (s, 3H), 1.20 (s, 3H), 1.16 (t, *J* = 7.2, 3H); ^{13}C NMR (100.6 MHz, d6-DMSO) δ 165.2, 161.7, 159.3, 143.0, 142.9, 139.1, 132.0, 128.2, 125.4, 113.2, 45.0, 34.5, 34.4, 33.4, 33.3, 31.5, 31.4, 31.2, 16.9, 12.3; IR (neat) 2952, 1663, 1591, 1508, 1426, 1281 cm^{-1}; ES-MS (M-H)- calcd for $C_{22}H_{28}N_3O_2$ 366.2181, found 366.2185. Anal. Calcd for $C_{22}H_{29}N_3O_2$: C, 71.90; H, 7.95; N, 11.43. Found: C, 71.81; H, 8.23; N, 11.31.

5-(Ethyl(5,5,8,8-tetramethyl-5,6,7,8-tetrahydronaphthalen-2-yl)amino)pyrazine-2-carboxylic acid (26). The same methodology to synthesize **20** gave **26** (0.2516 g, 71%) as a white crystalline solid, m.p. 213.1-214.4 °C: ^{1}H NMR (400 MHz, d6-DMSO) δ 12.59 (br s, 1H), 8.70 (d, *J* = 1.6, 1H), 7.61 (d, *J* = 1.2, 1H), 7.47 (d, *J* = 8.0, 1H), 7.29 (d, *J* = 2.4, 1H), 7.10 (dd, *J* = 8.4, 2.4, 1H), 3.94 (q, *J* = 7.1, 2H), 1.66 (s, 4H), 1.27 (s, 6H), 1.23 (s, 6H), 1.14 (t, *J* = 7.2, 3H); ^{13}C NMR (100.6 MHz, d6-DMSO) δ 165.4, 154.4, 146.7, 144.6, 143.8, 139.2, 130.8, 130.7, 128.4, 125.2, 124.4, 44.9, 34.4, 34.4, 34.1, 33.8, 31.5, 31.4, 12.2; IR (neat) 2931, 1671, 1556, 1416, 1276 cm^{-1}; ES-MS (M-H)- calcd for $C_{21}H_{26}N_3O_2$ 352.2025, found 352.2020. Anal. Calcd for $C_{21}H_{27}N_3O_2$: C, 71.36; H, 7.70; N, 11.89. Found: C, 70.43; H, 7.64; N, 11.61.

5-(Ethyl(3,5,5,8,8-pentamethyl-5,6,7,8-tetrahydronaphthalen-2-yl)amino)pyrazine-2-carboxylic acid (27). The same methodology to synthesize **20** gave pure **27** as a white crystalline solid, m.p. 203.6-205.1 °C: ^{1}H NMR (400 MHz, d6-DMSO) δ 12.69 (br s, 1H), 8.70 (s, 1H), 7.36 (br s, 2H), 7.15 (s, 1H), 4.15-4.05 (m, 1H), 3.59 (sextet, *J* = 7.2, 1H), 2.03 (s, 3H), 1.65 (s, 4H), 1.29, (s, 3H), 1.26 (s, 3H), 1.22 (s, 3H), 1.20 (s, 3H), 1.15 (t, *J* = 7.2, 3H); ^{13}C NMR (100.6 MHz, d6-DMSO) δ 165.4, 154.2, 144.8, 144.4, 144.3, 137.6, 132.3, 130.8, 130.0, 129.5, 126.4, 44.1, 34.5, 34.4, 33.7, 31.6. 31.5, 16.8, 12.1; IR (neat) 2959, 1671, 1557, 1524, 1417, 1286 cm^{-1}; ES-MS (M-H)- calcd for $C_{22}H_{28}N_3O_2$ 366.2181, found 366.2179. Anal. Calcd for $C_{22}H_{29}N_3O_2$: C, 71.90; H, 7.95; N, 11.43. Found: C, 71.62; H, 8.21; N, 11.19.

4-(Ethyl(5,5,8,8-tetramethyl-5,6,7,8-tetrahydronaphthalen-2-yl)amino)-2-fluorobenzoic acid (28). The same methodology to synthesize **20** gave pure **28** as a white crystalline solid, m.p. 252.4-256.8 °C: ^{1}H NMR (400 MHz, d6-DMSO) δ 12.35 (br s, 1H), 7.62 (t, *J* = 9.2, 1H), 7.41 (d, *J* = 8.4, 1H), 7.14 (d, *J* = 2.4, 1H), 6.97 (dd, *J* = 8.4, 2.4, 2H), 6.38 (dd, *J* = 9.2, 2.4, 1H), 6.32 (dd, *J* = 14.8, 2.4, 1H), 3.71 (q, *J* = 7.2, 2H), 1.65 (s, 4H), 1.26, (s, 6H), 1.21 (s, 6H), 1.12 (t, *J* = 7.2, 3H); ^{13}C NMR (100.6 MHz, d6-DMSO) δ 164.9, 164.8, 164.5, 161.9, 153.0 152.9, 146.4, 142.7, 141.9, 133.2, 128.1, 125.1, 124.5, 108.6, 105.7, 105.6, 99.7, 99.4, 46.3, 34.5, 34.4, 34.0, 33.7, 31.5, 31.4, 12.0; IR (neat) 2964, 1668, 1617, 1282 cm^{-1}; ES-MS (M-H)- calcd for $C_{23}H_{27}FNO_2$ 368.2026, found 368.2043. Anal. Calcd for $C_{23}H_{28}FNO_2$: C, 74.77; H, 7.64; N, 3.79; F, 5.14. Found: C, 74.42; H, 8.00; N, 3.64; F, 4.1.

Methyl 2-fluoro-4-((3,5,5,8,8-pentamethyl-5,6,7,8-tetrahydronaphthalen-2-yl)amino)-benzoate (65). The same methodology to synthesize **43** gave **65** (1.9009 g, 65%) as a crystalline solid, m.p. 159.7-165.1 °C: ^{1}H NMR (400 MHz, $CDCl_3$) δ 7.79 (t, *J* = 8.8, 1H), 7.17 (d, *J* = 3.6, 1H), 6.51 (dd, *J* = 8.8, 2.0, 1H), 6.38 (dd, *J* = 13.6, 2.0 1H), 5.74 (br s, 1H), 3.87 (s, 3H), 2.17 (s, 3H), 1.68 (s, 4H), 1.29 (s, 6H), 1.24 (s, 6H); ^{13}C NMR (100.6 MHz, $CDCl_3$) δ 165.3, 165.0, 164.9, 162.7, 151.9, 151.8, 143.9, 142.6, 135.2, 133.6, 133.5, 129.9, 129.1, 122.5, 109.6, 109.5, 107.5, 107.4, 100.9, 100.6, 51.7, 35.0. 34.9, 34.0, 33.9, 31.8; IR (neat) 3346, 2922, 1698, 1606, 1264 cm^{-1}; ES-MS (M+Na)+ calcd for $C_{23}H_{28}FNO_2Na$ 392.2002, found 392.2003.

4-(Ethyl(3,5,5,8,8-pentamethyl-5,6,7,8-tetrahydronaphthalen-2-yl)amino)-2-fluorobenzoic acid (29). The same methodology to synthesize **20** gave pure **29** as a white crystalline solid, m.p. 241.4-243.8 °C: ^{1}H NMR (400 MHz, d6-DMSO) δ 12.29 (br s, 1H), 7.62 (t, *J* = 8.8, 1H), 7.31 (s, 1H), 7.03 (s, 1H), 6.19-6.11 (m, 2H), 3.61 (br s, 2H), 1.98 (s, 3H), 1.63 (s, 4H), 1.26, (s, 6H), 1.20 (s, 6H), 1.13 (t, *J* = 7.2, 3H); ^{13}C NMR (100.6 MHz, d6-DMSO) δ 164.9, 164.9, 164.7, 162.2, 153.0, 152.9, 144.1, 143.7, 140.0, 133.4, 132.6, 129.3, 126.5, 107.3, 105.1, 105.0, 98.3, 98.0, 45.6, 34.5, 34.4, 33.7, 31.6, 31.5, 16.9, 12.1; IR (neat) 2922, 1670, 1606, 1285 cm^{-1}; ES-MS (M-H)- calcd for $C_{24}H_{29}FNO_2$ 382.2182, found 382.2170. Anal. Calcd for $C_{24}H_{30}FNO_2$: C, 75.16; H, 7.88; N, 3.65; F, 4.95. Found: C, 75.28; H, 8.45; N, 3.61; F, 4.3.

4-(1-(3,5,5,8,8-pentamethyl-5,6,7,8-tetrahydronaphthalen-2-yl)vinyl)benzenesulfonic acid (30). To a 100 mL round-bottomed flask equipped with a magnetic stir bar and charged with **71** (0.2046 g, 0.464 mmol) in methanol (3.0 mL) was added a solution of potassium hydroxide (0.0902 g, 1.61 mmol) in water (0.18 mL). The flask was fitted with a water condenser, and

heated to reflux in an oil bath at 85 °C for 2 h. The reaction was cooled to room temperature and 20% HCl (30 mL) was added. The resulting solution was extracted with ethyl acetate (50 mL, twice), and the combined organic layers were dried over sodium sulfate, filtered, concentrated *in vacuo* and purified by column chromatography (25 mL SiO_2, 10% methanol:ethyl acetate) to give **30** (0.1436 g, 80%) as a white crystalline solid, decomp. > 280 °C: ^{1}H NMR (400 MHz, d6-DMSO) δ 7.55 (d, *J* = 8.4, 2H), 7.18 (d, *J* = 8.4, 2H), 7.13 (s, 1H), 7.05 (s, 1H), 5.79 (d, *J* = 1.2, 1H), 5.14 (d, *J* = 1.2, 1H), 1.91 (s, 3H), 1.64 (s, 4H), 1.26 (s, 6H), 1.22 (s, 6H); ^{13}C NMR (100.6 MHz, d6-DMSO) δ 148.5, 147.4, 143.5, 141.7, 140.2, 138.2, 132.1, 127.7, 127.2, 125.7, 125.4, 115.4, 34.7, 34.6, 33.6, 33.4, 31.7, 31.6, 19.5; IR (neat) 2961, 1455, 1179, 1043, 1008, 845, 669 cm^{-1}; ES-MS (M-H)- calcd for $C_{23}H_{27}SO_3$ 383.1681, found 383.1667. Anal. Calcd for $C_{23}H_{28}O_4S\cdot(H_2O)_2$: C, 65.68; H, 7.67; S, 7.62. Found: C, 63.94; H, 7.35; S, 7.15.

4-(3,5,5,8,8-pentamethyl-5,6,7,8-tetrahydronaphthalene-2-carbonyl)benzenesulfonic acid (31). To a 20 dram vial charged with **69** (0.5621 g, 1.39 mmol) was added acetone (2.0 mL) and the vial was gently heated until the solution was homogeneous. To this solution of **69** in acetone was added a solution of potassium hydroxide (0.213 g, 3.80 mmol) in water (0.25 mL). The reaction was stirred and gently warmed to keep the solution homogeneous for 30 min at which point the reaction was quenched with 20% HCl (20 mL) and extracted with ethyl acetate (50 mL, thrice). The combined organic layers were washed with water (50 mL) and then brine (50 mL), dried over sodium sulfate, filtered, and concentrated *in vacuo* to give a crude produce that was purified by column chromatography (25 mL SiO_2, 10% methanol:ethyl acetate) to give **31** (0.300 g, 56%) as a white crystalline solid, decomp. > 200 °C: ^{1}H NMR (400 MHz, d6-DMSO) δ 7.75 (dd, *J* = 6.4, 1.6, 2H), 7.66 (dd, *J* = 6.4, 1.6, 2H), 7.30 (s, 1H), 7.21 (s, 1H), 2.21 (s, 3H), 1.65 (s,

4H), 1.28 (s, 6H), 1.18 (s, 6H); ^{13}C NMR (100.6 MHz, d6-DMSO) δ 197.1, 152.3, 147.1, 141.4, 137.3, 135.3, 133.2, 129.4, 128.9, 127.0, 125.8, 34.4, 34.3, 33.9, 33.5, 31.4, 31.3, 19.3; IR (neat) 2925, 1673, 1191, 1123, 1038 cm^{-1}; ES-MS (M-H)- calcd for $C_{22}H_{25}SO_4$ 385.1474, found 385.1472. Anal. Calcd for $C_{22}H_{26}O_4S\cdot(H_2O)_2$: C, 62.54; H, 7.16; S, 7.59. Found: C, 61.75; H, 6.76; S, 7.25.

ANCILLARY INFORMATION

Supporting Information

Full experimental details for the synthesis of **20**-**31** and all synthetic intermediates—**33**, **35**, **36**, **38**, **39**, **41**-**44**, **46**-**48**, **50**, **51**, **53**, **54**, **56**, **57**, **59**, **60**, **62**-**66**, and **68**-**71**—are provided in addition to ^{1}H-NMR and ^{13}C-NMR spectra as well as X-ray data for compounds **20**, **21**, **26**, **28**, **44**, and **60**. CCDC numbers 1480108 - 1480113 contain the supplementary crystallographic data for this work. These data can be obtained free of charge from The Cambridge Crystallographic Data Centre via www.ccdc.cam.ac.uk/data_request/cif.

Acknowledgements

We thank the Thome Foundation and the US National Institutes of Health for financial support of this work (R15 CA139364). We also thank Arizona State University's Women and Philanthropy grant program support. Thanks are also given to John Greaves of the High-Resolution Mass Spectrometry Laboratory at University of California, Irvine (UCI). Computer time was provided by USF Research Computing, sponsored in part by NSF MRI CHE-1531590 to AvdV. Patent applications covering the technologies described in this work have been applied for on behalf of the Arizona Board of Regents.

***Corresponding Author**: School of Mathematical and Natural Sciences, New College of Interdisciplinary Arts and Sciences, Arizona State University, 4701 W. Thunderbird Road, Glendale, AZ 85306. Tele: (602) 543-6087. Fax: (602) 543-6073. E-mail: Peter.Jurutka@asu.edu.

Abbreviations: CR, index of cross reactivity of RAR and RXR; CTCL, cutaneous T-cell lymphoma; HDAC, histone deacetylase; HDACi, histone deacetylase inhibitor; HRE, hormone responsive element; LBD, ligand binding domain; LXR, liver X receptor; LR, lipid risk assessment index; NaBu, sodium butyrate; NR, nuclear receptor; PPAR, peroxisome proliferator activating receptor; POC, proof of concept; RAR, retinoic-acid-receptor; RXR, retinoid-X-receptor; RXRE, retinoid-X-receptor element; SNuRMs, specific nuclear receptor modulators; SREBP sterol regulatory element-binding protein; TR, thyroid hormone receptor; VDR, vitamin D receptor.

References

[1] (a) Mangelsdorf, D.J.; Umesono, K.; Evans, R.M. The Retinoid Receptors, in *The Retinoids*; Academic Press: Orlando, FL, 1994; pp. 319-349. (b) Leid, M.; Kastner, P.; Chambon, P. Multiplicity Generates Diversity in the Retinoic Acid Signaling Pathways. *Trends Biochem. Sci.* **1992**, *17*, 427-433.

[2] Olefsky, J. M. Nuclear Receptor Minireview Series, *J. Biol. Chem.* **2001**, *276*(40), 36863-36864.

[3] (a) Perlmann, T.; Rangarahan, P.N.; Umesono, K.; Evans, R.M. Determinants for Selective RAR and TR Recognition of Direct Repeat HREs. *Genes Dev.*, **1993**, *7*(7B), 1411-1422. (b) Phan, T.Q.; Jow, M.M.; Privalsky, M.L. DNA Recognition by Thyroid Hormone and Retinoic Acid Receptors: 3-4-5 Rule Modified. *Mol. Cell Endocrinol.*, **2010**, *319*(1-2), 88-98.

[4] Forman, B. M.; Yang, C.-R.; Au, M.; Casanova, J.; Ghysdael, J.; Samuels, H. H. A Domain Containing Leucine-zipper-like Motifs Mediates Novel *in vitro* Interactions between the Thyroid Hormone and Retinoic Acid Receptors. *Mol. Endocrinol.* **1989**, *3*, 1610-1626.

[5] Mangelsdorf, D. J.; Evans, R. M. The RXR Heterodimers and Orphan Receptors. *Cell* **1995**, *83***,** 841-850.

[6] Thompson, P. D.; Remus, L. S.; Hsieh, J.-C.; Jurutka, P. W.; Whitfield, G. K.; Galligan, M. A.; Encinas Dominguez C.; Haussler, C. A.; Haussler, M. R. Distinct Retinoid X Receptor Activation Function-2 Residues Mediate Transactivation in Homodimeric and Vitamin D Receptor Heterodimeric Contexts. *J. Mol. Endocrinol.* **2001**, *27*(2)**,** 211-227.

[7] Svensson, S.; Ostberg, T.; Jacobsson, M.; Norstrom, C.; Stefansson, K.; Hallen, D.; Johansson, I.C.; Zachrisson, K.; Ogg, D.; Jendeberg, L. Crystal Structure of the Heterodimeric Complex of

LXRα and RXRβ Ligand-binding Domains in a Fully Agonistic Conformation. *EMBO J.* **2003**, *22*, 4625-4633.

[8] Nahoum, V.; Perez, E.; Germain, P.; Rodriquez-Barrios, F.; Manzo, F.; Kammerer, S.; Lemaire, G.; Hirsch, O.; Royer, C.A.; Gronemeyer, H.; de Lera, A.R.; Bourguet, W. Modulators of the Structural Dynamics of the Retinoid X Receptor to Reveal Receptor Function. *PNAS*, **2007**, *104*, 17323-17328.

[9] Forman, B.M.; Umesono, K.;Chen, J.; Evans, R.M. Unique Response Pathways are Established by Allosteric Interactions Among Nuclear Hormone Receptors." *Cell* **1995**, *81*, 541-550.

[10] Lala, D.S.; Mukherjee, R.; Schulman, I.G.; Canan Koch, S.S.; Dardashti, L.J.; Nadzan, A.M.; Croston, G.E.; Evans, R.M.; Heyman, R.A. Activation of Specific RXR Heterodimers by an Antagonist of RXR Homodimers. *Nature* **1996**, *383*, 450–453.

[11] (a) Lemon, B.D.; Freedman, L.P. Selective Effects of Ligands on Vitamin D3 Receptor- and Retinoid X Receptor-mediated Gene Activation In Vivo. *Mol. Cell. Biol.* **1996**, *16*, 1006-1016 (b) MacDonald, P.N.; Dowd, D.R.; Nakajima, S.; Galligan, M.A.; Reeder, M.C.; Haussler, C.A.; Ozato, K.; Haussler, M.R. Retinoid X Receptors Stimulate and 9-Cis Retinoic Acid Inhibits 1,25-Dihydroxyvitamin D3-activated Expression of the Rat Osteocalcin Gene. *Mol. Cell. Biol.* **1993**, *13*, 5907–5917. (c) Thompson, P.D.; Jurutka, P.W.; Haussler, C.A.; Whitfield, G.K.; Haussler, M.R. Heterodimeric DNA Binding by the Vitamin D Receptor and Retinoid X Receptors is Enhanced by 1,25-Dihydroxyvitamin D3 and Inhibited by 9-Cis Retinoic Acid: Evidence for Allosteric Receptor Interactions. *J. Biol. Chem.* **1998**, *273*, 8483-8491.

[12] Lehmann, J.M; Zhang, X.K.; Graupner, G.; Lee, M.O.; Hermann, T.; Hoffmann, B.; Pfahl, M. Formation of Retinoid X Receptor Homodimers Leads to Repression of T3 Response: Hormonal Cross Talk by Ligand-Induced Squelching. *Mol. Cell. Biol.* **1993**, *13*, 7698-7707.

[13] (a) Raval-Pandya, M.; Freedman, L.P.; Li, H.; Christakos, S. Thyroid Hormone Receptor Does Not Heterodimerize with the Vitamin D Receptor but Represses Vitamin D Receptor-Mediated Transactivation. *Mol. Endocrinol.* **1998**, *12*, 1367-1379. (b) Thompson, P.D.; Hsieh, J.-C.; Whitfield, G.K.; Haussler, C.A.; Jurutka, P.W.; Galligan, M.A.; Tillman, J.B.; Spindler, S.R.; Haussler, M.R. Vitamin D Receptor Displays DNA Binding and Transactivation as a Heterodimer with the Retinoid X Receptor, but not with the Thyroid Hormone Receptor. J. *Cell. Biochem.* **1999**, *75*, 462-480.

[14] Yen, P.M.; Liu, Y.; Sugawara, A.; Chin, W.W. Vitamin D Receptors Repress Basal Transcription and Exert Dominant Negative Activity on Triiodothyronine-mediated Transcriptional Activity. *J. Biol. Chem.* **1996**, *271*, 10910-10916.

[15] Altucci, L.; Leibowitz, M. D.; Ogilvie, K. M.; de Lera, A. R.; Gronemeyer, H. RAR and RXR Modulation in Cancer and Metabolic Disease. *Nature Rev. Drug Discov.* **2007**, *6*, 793-810.

[16] Lehmann, J.M.; Jong, L.; Fanjul, A.; Cameron, J.F.; Lu, X.-P.; Haefner, P.; Dawson, M.I.; Pfahl, M. Retinoids Selective for Retinoid X Receptor Pathways. *Science* **1992**, *258*, 1944-1946.

[17] (a) Jong, L.; Lehmann, J. M.; Hobbs, P. D.; Harlev, E.; Huffman, J. C.; Pfahl, M.; Dawson, M. I. Conformational Effects on Retinoid Receptor Selectivity. 1. Effect of 9-Double Bond Geometry on Retinoid X Receptor Activity. *J. Med. Chem.* **1993**, *36*, 2605-2613. (b) Dawson, M.I.; Jong, L.; Hobbs, P.D.; Cameron, J.F.; Chao, W.-R.; Pfahl, M.; Lee, M.-O.; Shroot, B.; Pfahl, M. Conformational Effects on Retinoid Receptor Selectivity. 2. Effects of Retinoid

Bridging Group on Retinoid X Receptor Activity and Selectivity. *J. Med. Chem.* **1995**, *38*, 3368-3383.

[18] Boehm, M.F.; Zhang, L.; Badea, B.A.; White, S.K.; Mais, D.E.; Berger, E.; Suto, C.M.; Goldman, M.E.; Heyman, R.A. Synthesis and Structure-Activity Relationships of Novel Retinoid X Receptor-Selective Retinoids. *J. Med. Chem.* **1994**, *37*, 2930-2941.

[19] Daiss, J.O.; Burschka, C.; Mills, J.S.; Montana, J.G.; Showell, G.A.; Fleming, I.; Gaudon, C.; Ivanova, D.; Gronemeyer, H.; Tacke, R. Synthesis, Crystal Structure Analysis, and Pharmacological Characterization of Disila-bexarotene, a Disila-Analogue of the RXR-Selective Retinoid Agonist Bexarotene. *Organometallics* **2005**, *24*, 3192-3199.

[20] Cesario, R. M.; Stone, J.; Yen, W.-C.; Bissonnette, R. P.; Lamph, W. W. Differentiation and Growth Inhibition Mediated via the RXR:PPAR$_\gamma$ Heterodimer in Colon Cancer. *Cancer Letters* **2006**, *240*, 225-233.

[21] Yen, W. -C.; Prudente, R. Y.; Lamph, W. W. Synergistic Effect of a Retinoid X Receptor-Selective Ligand Bexarotene (LGD1069, Targretin) and Paclitaxel (Taxol) in Mammary Carcinoma. *Breast Cancer Res. Treat.* **2004**, *88*, 141-148.

[22] (a) Yen, W.-C.; Corpuz, M. R.; Prudente, R. Y.; Cooke, T. A.; Bissonnette, R. P.; Negro-Vilar, A.; Lamph, W. W. A Selective Retinoid X Receptor Agonist Bexarotene (Targretin) Prevents and Overcomes Acquired Paclitaxel (Taxol) Resistance in Human Non-Small Cell Lung Cancer. *Clin. Cancer Res.* **2004**, *10*, 8656-8664. (b) Dragnev, K.H.; Petty, W.J.; Shah, S.J.; Lewis, L.D.; Black, C.C.; Memoli, V.; Nugent, W.C.; Hermann, T.; Negro-Vilar, A.; Rigas, J.R.; Dmitrovsky, E. A Proof-of-Principle Clinical Trial of Bexarotene in Patients with Non-Small Cell Lung Cancer. *Clin. Cancer Res.* **2007**, *13*, 1794-1800.

[23] Mukherjee, R.; Davies, P. J. A.; Crombie, D. L.; Bischoff, E. D.; Cesario, R. M.; Jow, L.; Hamanns, L. G.; Boehm, M. F.; Mondon, C. E.; Nadzan, A. M.; Paterniti, J. R.; Heyman, R. A. Sensitization of Diabetic and Obese Mice to Insulin by Retinoid X Receptor Agonists. *Nature* **1997**, *386*, 407-410.

[24] Sherman, S. I.; Gopal, J.; Haugen, B. R.; Chiu, A. C.; Whaley, K.; Nowlakha, P.; Duvic, M. Central Hypothyroidism Associated with Retinoid X Receptor-selective Ligands. *N. Engl. J. Med.* **1999**, *340*, 1075-1079.

[25] Li, D.; Li, T.; Wang, F.; Tian, H.; Samuels, H. H. Functional Evidence for Retinoid X Receptor (RXR) as a Nonsilent Partner in the Thyroid Hormone Receptor/RXR Heterodimer. *Mol. Cell. Biol*. **2002**, *22*, 5782-5792.

[26] (a) Murthy, S.; Born, E.; Mathur, S.N.; Field, F.J. LXR/RXR Activation Enhances Basolateral Efflux of Cholesterol in CaCo-2 Cells. *J. Lipid Res.* **2002**, *43*, 1054-1064. (b) Field, F.J.; Born, E.; Mathur, S.N. LXR/RXR Ligand Activation Enhances Basolateral Efflux of Beta-sitosterol in CaCo-2 Cells. *J. Lipid Res.* **2004**, *45*, 905-913.

[27] Thacher, S. M.; Standeven, A.M.; Athanikar, J.; Kopper, S.; Castilleja, O.; Escobar, M.; Beard, R.L.; Chandraratna, R.A.S. Receptor Specificity of Retinoid-Induced Epidermal Hyperplasia: Effect of RXR-Selective Agonists and Correlation with Topical Irritation. *JPET* **1997**, *282*, 528-534.

[28] McFarland, K.; Spalding, T.A.; Hubbard, D.; Ma, J.-N.; Olsson, R.; Burstein, E.S. Low Dose Bexarotene Treatment Rescues Dopamine Neurons and Restores Behavioral Function in Models of Parkinson's Disease. *ACS Chem. Neurosci.* **2013**, *4*(11), 1430-1438.

[29] (a) Cramer, P.E.; Cirrito, J.R.; Wesson, D.W.; Lee, C.Y.D.; Karlo, J.C.; Zinn, A.E.; Casali, B.T.; Restivo, J.L.; Goebel, D.A.; James, M.J.; Brunden, K.R.; Wilson, D.A.; Landreth, G.E. ApoE-Directed Therapeutics Rapidly Clear β-Amyloid and Reverse Deficits in AD Mouse Models. *Science* **2012**, *335*, 1503-1506. (b) Landreth, G.E.; Cramer, P.E.; Lakner, M.M.; Cirrito, J.R.; Wesson, D.W.; Brunden, K.R.; Wilson, D.A. Response to Comments on 'ApoE-Directed Therapeutics Rapidly Clear β-Amyloid and Reverse Deficits in AD Mouse Models'. *Science* **2013**, *340*, 924.

[30] Cummings, J.L.; Zhong, K.; Kinney, J.W.; Heany, C.; Moll-Tudla, J.; Joshi, A.; Pontecorvo, M.; Devous, M.; Tang, A.; Bena, J. Double-blind, Placebo-controlled, Proof-of-concept trial of Bexarotene Xin Moderate Alzheimer's Disease. *Alzheimer's Research & Therapy* **2016**, *8*:4 DOi 10.1186/s13195-016-0173-2.

[31] Vuligonda, V.; Thacher, S. M.; Chandraratna, R. A. S. Enantioselective Synthesis of Potent Retinoid X Receptor Ligands: Differential Biological Activities of Individual Antipodes. *J. Med. Chem.* **2001**, *44*, 2298-2303.

[32] (a) Muccio, D.D.; Brouillette, W.J.; Breitman, T.R.; Taimi, M.; Emanuel, P.D.; Zhang, X.; Chen, G.; Sani, B.P.; Venepally, P.; Reddy, L.; Alam, M.; Simpson-Herren, L.; Hill, D.L. Conformationally Defined Retinoic Acid Analogues 4. Potential New Agents for Acute Promyelocytic and Juvenile Myelomonocytic Leukemias. *J. Med. Chem.* **1998**, *41*, 1679-1687.

[33] (a) Atigadda, V.R.; Vines, K.K.; Grubbs, C.J.; Hill, D.L.; Beenken, S.L.; Bland, K.I.; Brouillette, W.J.; Muccio, D.D. Conformationally Defined Retinoic Acid Analogues. 5. Large-Scale Synthesis and Mammary Cancer Chemopreventive Activity for (2E,4E,6Z,8E)-8-(3',4'-Dihydro-1'(2'H)-naphthalen-1'-ylidene)-3,7-dimethyl-2,4,6-octatrienoic Acid (9cUAB30). *J. Med. Chem.* **2003**, *46*(17), 3766-3769. (b) Kolesar, J.M.; Hoel, R.; Pomplun, M.; Havighurst, T.;

Stublaski, J.; Wollmer, B.; Krontiras, H.; Brouillette, W.; Muccio, D.; Kim, K.; Grubbs, C.J.; Bailey, H.E. A Pilot, First-in-human, Pharmacokinetic Study of 9cUAB30 in Healthy Volunteers. *Cancer Prev. Res.* **2010**, *55*, 4489-4500. (c) Hansen, N.J.; Wylie, R.C.; Phipps, S.M.O.; Love, W.K.; Andrews, L.G.; Tollefsbol, T.O. The Low-toxicity 9-cis UAB30 Novel Retinoids Down-regulates the DNA Methyltransferases and has Anti-telomerase Activity in Human Breast Cancer Cells. *International Journal of Oncology* **2007**, *30*, 641-650.

[34] (a) Atigadda, V.R.; Xia, G.; Desphande, A.; Boerma, L.J.; Lobo-Ruppert, S.; Grubbs, C.J.; Smith, C.D.; Brouillette, W.J.; Muccio, D.D. Methyl Substitution of a Rexinoid Agonist Improves Potency and Reveals Site of Lipid Toxicity. *J. Med. Chem.* **2014**, *57*, 5370-5380. (b) Desphande, A.; Xia, G.; Boerma, L.J.; Vines, K.K.; Atigadda, V.R.; Lobo-Ruppert, S.; Grubbs, C.J.; Moeinpour, F.L.; Smith, C.D.; Christov, K.; Brouillette, W.J.; Muccio, D.D. Methyl-Substituted Conformationally Constrained Rexinoid Agonists for the Retinoid X Receptors Demonstrate Improved Efficacy for Cancer Therapy and Prevention. *Bioorg. Med. Chem.* **2014**, *22*(1), 178-185.

[35] Michellys, P. Y.; Ardecky, R. J.; Chen, J. H.; Crombie, D. L.; Etgen, G. J.; Faul, M. M.; Faulkner, A. L.; Grese, T. A.; Heyman, R. A.; Karanewsky, D. S.; Klausing, K.; Leibowitz, M. D.; Liu, S.; Mais, D. A.; Mapes, C. M.; Marschke, K. B.; Reifel-Miller, A.; Ogilvie, K. M.; Rungta, D.; Thompson, A. W.; Tyhonas, J. S.; Boehm, M. F. Novel (2*E*,4*E*,6*Z*)-7-(2-Alkoxy-3,5-dialkylbenzene)-3-methylocta-2,4,6-trienoic Acid Retinoid X Receptor Modulators are Active in Models of Type 2 Diabetes. *J. Med. Chem.* **2003**, *46*, 2683-2696.

[36] Michellys, P.-Y.: Ardecky, R. J.; Chen, J.-H.; D'Arrigo, J.; Grese, T. A.; Karanewsky, D. S.; Leibowitz, M. D.; Liu, S.; Mais, D. A.; Mapes, C. M.; Montrose-Rafizadeh, C.; Ogilvie, K. M.;

Reifel-Miller, A.; Rungta, D.; Thompson, A. W.; Tyhonas, J. S.; Boehm, M. F. Design, Synthesis, and Structure-Activity Relationship Studies of Novel 6,7-Locked-[7-(2-alkoxy-3,5-dialkylbenzene)-3-methylocta]-2,4,6-trienoic Acids. *J. Med. Chem.* **2003**, *46*, 4087-4103.

[37] Michellys, P.-Y.; Darrigo, J.; Grese, T. A.; Karanewsky, D. S.; Leibowitz, M. D.; Mais, D. A.; Mapes, C. M.; Reifel-Miller, A.; Rungta, D.; Boehm, M. F. Design, Synthesis and Structure-Activity Relationship of Novel RXR-selective Modulators. *Bioorg. Med. Chem. Lett.* **2004**, *14*, 1593-1598.

[38] Wagner, C.E.; Jurutka, P.W.; Marshall, P.A.; Groy, T.L.; van der Vaart, A.; Ziller, J.W.; Furmick, J.K.; Graeber, M.E.; Matro, E.; Miguel, B.V.; Tran, I.T.; Kwon, J.; Tedeschi, J.N.; Moosavi, S.; Danishyar, A.; Philp, J.S.; Khamees, R.O.; Jackson, J.N.; Grupe, D.K.; Badshah, S.L.; Hart, J.W. Modeling, Synthesis and Biological Evaluation of Potential Retinoid X Receptor (RXR) Selective Agonists: Novel Analogues of 4-[1-(3,5,5,8,8-Pentamethyl-5,6,7,8-tetrahydro-2-naphthyl)ethynyl]benzoic Acid (Bexarotene). *J. Med. Chem.* **2009**, *52*, 5950-5966.

[39] Furmick, J.K.; Kaneko, I.; Walsh, A.N.; Yang, J.; Bhogal, J.S.; Gray, G.M.; Baso, J.C.; Browder, D.O.; Prentic, J.L.S.; Montano, L.A.; Huynh, C.C.; Marcus, L.M.; Tsosie, D.G.; Kwon, J.S.; Quezada, A.; Reyes, N.M.; Lemming, B.; Saini, P.; van der Vaart, A.; Groy, T.L.; Marshall, P.A.; Jurutka, P.W.; Wagner, C.E. Modeling, Synthesis and Biological Evaluation of Potential Retinoid X Receptor-Selective Agonists: Novel Halogenated Analogues of 4-[1-(3,5,5,8,8-Pentamethyl-5,6,7,8-tetrahydro-2-naphthyl)ethynyl]benzoic Acid (Bexarotene). *ChemMedChem*, **2012**, *7*, 1551-1566.

[40] Boehm, M.F.; Zhang, L.; Zhi, L.; McClurg, M.R.; Berger, E.; Wagoner, M.; Mais, D.E.; Suto, C.M.; Davies, P.J.A.; Heyman, R.A.; Nadzan, A.M. Design and Synthesis of Potent Retinoid X

Receptor Selective Ligands That Induce Apoptosis in Leukemia Cells. *J. Med. Chem.* **1995**, *38*, 3146-3155.

[41] Zhang, L.; Badea, B.A.; Enyeart, D.; Berger, E.M.; Mais, D.E.; Boehm, M.F. Synthesis of Isotopically Labeled 4-[1-(3,5,5,8,8-Pentamethyl-5,6,7,8-tetrahydro-2-naphthyl)ethenyl]benzoic Acid (LGD1069). *Journal of Labelled Compounds and Radiopharmaceuticals* **1995**, *36*, 701-712.

[42] Faul, M.M.; Ratz, A.M.; Sullivan, K.A.; Trankle, W.G.; Winneroski, L.L. Synthesis of Novel Retinoid X Receptor-Selective Retinoids. *J. Org. Chem.* **2001**, *66*, 5772-5782.

[43] Santin, E.P.; Germain, P.; Quillard, F.; Khanwalkar, H.; Rodriguez-Barrios, F.; Gronemeyer, H.; de Lera, A.R.; Bourguet, W. Modulating Retinoid X Receptor with a Series of (*E*)-3-[4-Hydroxy-3-(3-alkoxy-5,5,8,8-tetramethyl-5,6,7,8-tetrahydronaphthalen-2-yl)phenyl]acrylic Acids and Their 4-Alkoxy Isomers. *J. Med. Chem.* **2009**, *52*, 3150-3158.

[44] Gianni, M.; Ponzanelli, I.; Mologni, L.; Reichert, U.; Rambaldi, A.; Terao, M.; Garattini, E. Retinoid-dependent Growth Inhibition, Differentiation and Apoptosis in Acute Promyelocytic Leukemia Cells. Expression and Activation of Caspases. *Cell Death Differ.* **2000**, *7*, 447-460.

[45] Jurutka, P.W.; Kaneko, I.; Yang, J.; Bhogal, J.S.; Swierski, J.C.; Tabacaru, C.R.; Montano, L.A.; Huynh, C.C.; Jama, R.A.; Mahelona, R.D.; Sarnowski, J.T.; Marcus, L.M.; Quezada, A.; Lemming, B.; Tedesco, M.A.; Fischer, A.J.; Mohamed, S.A.; Ziller, J.W.; Ma, N.; Gray, G.M.; van der Vaart, A.; Marshall, P.A.; Wagner, C.E. Modeling, Synthesis, and Biological Evaluation of Potential Retinoid X Receptor (RXR) Selective Agonists: Novel Analogues of 4-[1-(3,5,5,8,8-Pentamethyl-5,6,7,8-tetrahydro-2-naphthyl)ethynyl]benzoic Acid (Bexarotene) and (*E*)-3-(3-(1,2,3,4-tetraydro-1,1,4,4,6-pentamethylnaphthalen-7-yl)-4-hydroxyphenyl)acrylic Acid (CD3254). *J. Med. Chem.* **2013**, *56*, 8432-8454.

[46] Marshall, P.A.; Jurutka, P.W.; Wagner, C.E.; van der Vaart, A.; Kaneko, I.; Chavez, P.I.; Ma, N.; Bhogal, J.S.; Shahani, P.; Swierski, J.C.; MacNeill, M. Analysis of Differential Secondary Effects of Novel Rexinoids: Select Rexinoid X Receptor Ligands Demonstrate Differentiated Side Effect Profiles" *Pharma. Res. Per.* **2015**, *3*(2), e00122, doi: 10.1002/prp2.122.

[47] (a) Fujii, S.; Ohsawa, F.; Yamada, S.; Shinozaki, R.; Fukai, R.; Makishima, M.; Enomoto, S.; Tai, A.; Kakuta, H. Modification at the Acidic Domain of RXR Agonists has Little Effect on Permissive RXR-heterodimer Activation. *Bioorg. Med. Chem. Lett.* **2010**, *20*(17), 5139-5142. (b) Ohsawa, F.; Morishita, K.-i.; Yamada, S.; Makishima, M.; Kakuta, H. Modification at the Lipophilic Domain of RXR Agonists Differentially Influences Activation of RXR Heterodimers. *ACS Med. Chem. Lett.* **2010**, *1*(9), 521-525. (c) Kakuta, H.; Yakushiji, N.; Shinozaki, R.; Ohsawa, F.; Yamada, S.; Ohta, Y.; Kawata, K.; Nakayama, M.; Hagaya, M.; Fujiwara, C.; Makishima, M.; Uno, S.; Tai, A.; Maehara, A.; Nakayama, M.; Oohashi, T.; Yasui, H.; Yoshikawa, Y. RXR Partial Agonist CBt-PMN Exerts Therapeutic Effects on Type 2 Diabetes without Side Effects of RXR Full Agonists. *ACS Med. Chem. Lett.* **2012**, *3*(5), 427-432. (d) Kakuta, H.; Ohsawa, F.; Yamada, S.; Makishima, M.; Tai, A.; Yasui, H.; Yoshikawa, Y. Feasibility of Structural Modification of Retinoid X Receptor Agonists to Separate Blood Glucose-lowering Action from Adverse Effects: Studies in KKAy Type 2 Diabetes Model Mice" *Biological & Pharmaceutical Bulletin* **2012**, *35*(4), 629-633. (e) Ohsawa, F.; Yamada, S.; Yakushiji, N.; Shinozaki, R.; Nakayama, M.; Kawata, K.; Hagaya, M.; Kobayashi, T.; Kohara, K.; Furusawa, Y.; Fujiwara, C.; Ohta, Y.; Makishima, M.; Naitou, H.; Tai, A.; Yoshikawa, Y.; Yasui, H.; Kakuta, H. Mechanism of Retinoid X Receptor Partial Agonistic Action of 1-(3,5,5,8,8-Pentamethyl-5,6,7,8-tetrahydro-2-naphthyl)-1H-benzotriazole-5-carboxylic Acid and Structural Development To Increase Potency. *J. Med. Chem.* **2013**, *56*(5), 1865-1877.

[48] (a) Ohta, K.; Tsuji, M.; Kawachi, E.; Fukasawa, H.; Hashimoto, Y.; Shudo, K.; Kagechika, H. Potent Retinoid Synergists with a Diphenylamine Skeleton. *Biological & Pharmaceutical Bulletin* **1998**, *21*(5), 544-546. (b) Kagechika, H.; Shudo, K.; Sugioka, T.; Sotome, T.; Nakayama, Y.; Doi, K. Preparation of Benzoic Acid Derivatives as Retinoid Activity Regulators. From PCT Int. Appl. (1998), WO 9845242 A1 19981015. (c) Ohta, K.; Kawachi, E.; Fukusawa, H.; Shudo, K.; Kagechika, H. Diphenylamine-based Retinoid Antagonists: Regulation of RAR and RXR Function Depending on the N-substituent. *Bioorg. Med. Chem.* **2011**, *19*(8), 2501-2507.

[49] The ThalesNano H-Cube® was used for this hydrogenation reaction.

[50] Egea, P.F.; Mitschler, A.; Moras, D. Molecular Recognition of Agonist Ligands by RXRs. *Mol. Endocrinol.* **2002**, *16*, 987-997.

[51] (a) Deng, N.; Forli, S; He, P.; Perryman, A.; Wickstrom, L.; Vijayan, R.S.; Tiefenbrunn, T.; Stout, D.; Gallicchio, E.; Olson, A.J.; Levy R.M. Distinguishing Binders from False Positives by Free Energy Calculations: Fragment Screening Against the Flap Site of HIV Protease. *J. Phys. Chem. B* **2015**, *119*(3), 976-988. (b) Durrant, J.D.; Amaro, R.E.; Xie, L.; Urbaniak, M.D.; Ferguson, M.A.J.; Haapalainen, A.; Chen, Z; Di Guilmi, A.M.; Wunder, F.; Bourne, P.E.; McCammon, J.A. A Multidimensional Strategy to Detect Polypharmacological Targets in the Absence of Structural and Sequence Homology. *PLoS Comp. Biol.* **2010**, *6*(1), e1000648.

[52] Wakelee, H.A.; Takimoto, C.H.; Lopez-Anaya, A.; Chu, Q.; Middleton, G.; Dunlop, D.; Ramlau, R.; Leighl, N.; Rowinsky, E.K.; Hao, D.; Zatloukai, P.; Jacobs, C.D.; Rodon, J. The Effect of Bexarotene on Atorvastatin Pharmacokinetics: Results from a Phase I Trial of

Bexarotene Plus Chemotherapy in Patients with Advanced Non-small Cell Lung Cancer." *Cancer Chemother. Pharmacol.* **2012**, *69*(2), 563-571.

[53] Yoon, S.; Eom, G.H. HDAC and HDAC Inhibitor: From Cancer to Cardiovascular Diseases. *Chonnam Med. J.* **2016**, *52*(1), 1-11.

[54] (a) Hong-Qi, Y.; Zhi-Kun, S.; Sheng-Di, C. Current Advances in the Treatment of Alzheimer's Disease: Focus on Considerations Targeting Aβ and Tau. *Translational Neurodegeneration* **2012** *1*:21. (b) Gross, M. Understanding Amyloid and Alzheimer's Disease. *Current Biology* **2012**, *22*(10), R381-R384. (c) Appleby, B.S.; Nacopoulos, D.; Milano, N.; Zhong, K.; Cummings, J.L. A Review: Treatment of Alzheimer's Disease Discovered in Repurposed Agents. *Dement. Geriatr. Cogn. Disord.* **2013**, *35*, 1-22.

[55] Hanwell, M.D.; Curtis, D.E.; Lonie, D.C.; Vandermeersch, T.; Zurek, E.; Hutchison, G.R. Avogadro: an Advanced Semantic Chemical Editor, Visualization, and Analysis Platform. *J. Cheminform.* **2012**, *13*(4), 17.

[56] Rappe, A.K.; Casewit, C.J.; Colwell, K.S.; Goddard, W.A.; Skiff, W.M UFF, a Full Periodic-table Force-field for Molecular Mechanics and Molecular-dynamics Simulations. *J. Am. Chem. Soc.*, **1992**, *114*, 10024-10035.

[57] Morris, G.M.; Huey, R.; Lindstrom, W.; Sanner, M.F.; Belew, R.K.; Goodsell, D.S.; Olson, A.J. AutoDock4 and AutoDock Tools4: Automated Docking with Selective Receptor Flexibility. *J. Comput. Chem.* **2009**, *30*, 2785-2791.

[58] O'Boyle, N.M; Banck, M.; James, C.A.; Morley, C.; Vandermeersch, T.; Hutchison, G.R. Open Babel: An Open Chemical Toolbox. *J. Cheminf.* **2011**, *3*, 33.

[59] Haffner, C.D.; Lenhard, J.M.; Miller, A.B.; McDougald, D.L.; Dwornik, K.; Ittoop, O.R.; Gampe, Jr., R.T.; Xu, H.E.; Blanchard, S.; Montana, V.G.; Consler, T.G.; Bledsoe, R.K.;

Ayscue, A.; Croom, D. Structure-based Design of Potent Retinoid X Receptor α Agonists. *J. Med. Chem.*, **2004**, *47*, 2010-2029.

[60] Lippert, W.P.; Burschka, C.; Gotz, K.; Kaupp, M.; Ivanova, D.; Gaudon, C.; Sato, Y.; Antony, P.; Rochel, N.; Moras, D.; Gronemeyer, H.; Tacke, R. Silicon Analogues of the RXR-selective Retinoid Agonist SR11237 (BMS649): Chemistry and Biology. *ChemMedChem*, **2009**, *4*, 1143-1152.

[61] Chandra, V.; Huang, P.; Hamuro, Y.; Raghuram, S.; Wang, Y.; Burris, T.P.; Rastinejad, F. Structure of the Intact PPAR-γ-RXR-α Nuclear Receptor Complex on DNA. *Nature*, **2008**, *456*, 350-356.

[62] Connors, R.V.; Wang, Z.; Harrison, M.; Zhang, A.; Wanska, M.; Hiscock, S.; Fox, B.; Dore, M.; Labelle, M.; Sudom, A.; Johnstone, S.; Liu, J.; Walker, N.P.; Chai, A.; Siegler, K.; Li, Y.; Coward, P. Identification of a PPARδ Agonist with Partial Agonistic Activity on PPARγ. *Bioorg. Med. Chem. Lett.*, **2009**, *19*, 3550-3554.

[63] Zhang, Y.; Zhang, H.; Yao, X.G.; Shen, H.; Chen, J.; Li, C.; Chen, L.; Zheng, M.; Ye, J.; Hu, L.; Shen, X.; Jiang, H. (+)-Rutamarin as a Dual Inducer of Both GLUT4 Translocation and Expression Efficiently Ameliorates Glucose Homeostasis in Insulin-resistant Mice. *PloS one*, **2012**, *7*, e31811.

[64] Love, J.D.; Gooch, J.T.; Benko, S.; Li, C.; Nagy, L.; Chatterjee, V.K.; Evans, R.M.; Schwabe, J.W. The Structural Basis for the Specificity of Retinoid-X Receptor-selective Agonists: New Insights into the Role of Helix H12. *J. Biol. Chem.*, **2002**, *277*, 11385-11391.

[65] (a) Zimmerman, F.K. Procedures Used in the Induction of Mitotic Recombination and Mutation in the Yeast *Saccharomyces cerevisiae*. *Mutat. Res.* **1975**, *31*, 71-86. (b) Zimmermann,

F.K.; Kern, R.; Rasenberger, H. A Yeast Strain for Simultaneous Detection of Mitotic Crossing Over, Mitotic Gene Conversion, and Reverse Mutation. *Mutat. Res.* **1975**, *28*, 381-388.

[66] Marshall, P.A. Using *Saccharomyces cerevisiae* to Test the Mutagenicity of Household Compounds: An Open Ended Hypothesis-Driven Teaching Lab. *CBE-LSE* **2007**, *6*, 307-315.

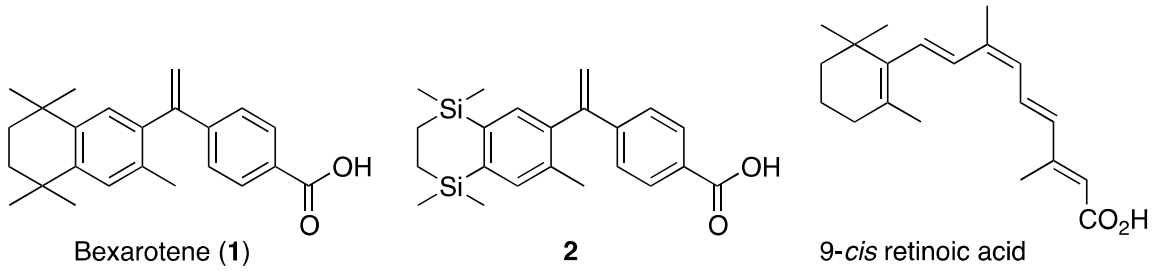

Bexarotene (**1**) **2** 9-*cis* retinoic acid

Figure 1. Two synthetic rexinoids, **1** and **2**, modeled after 9-*cis* retinoic acid.

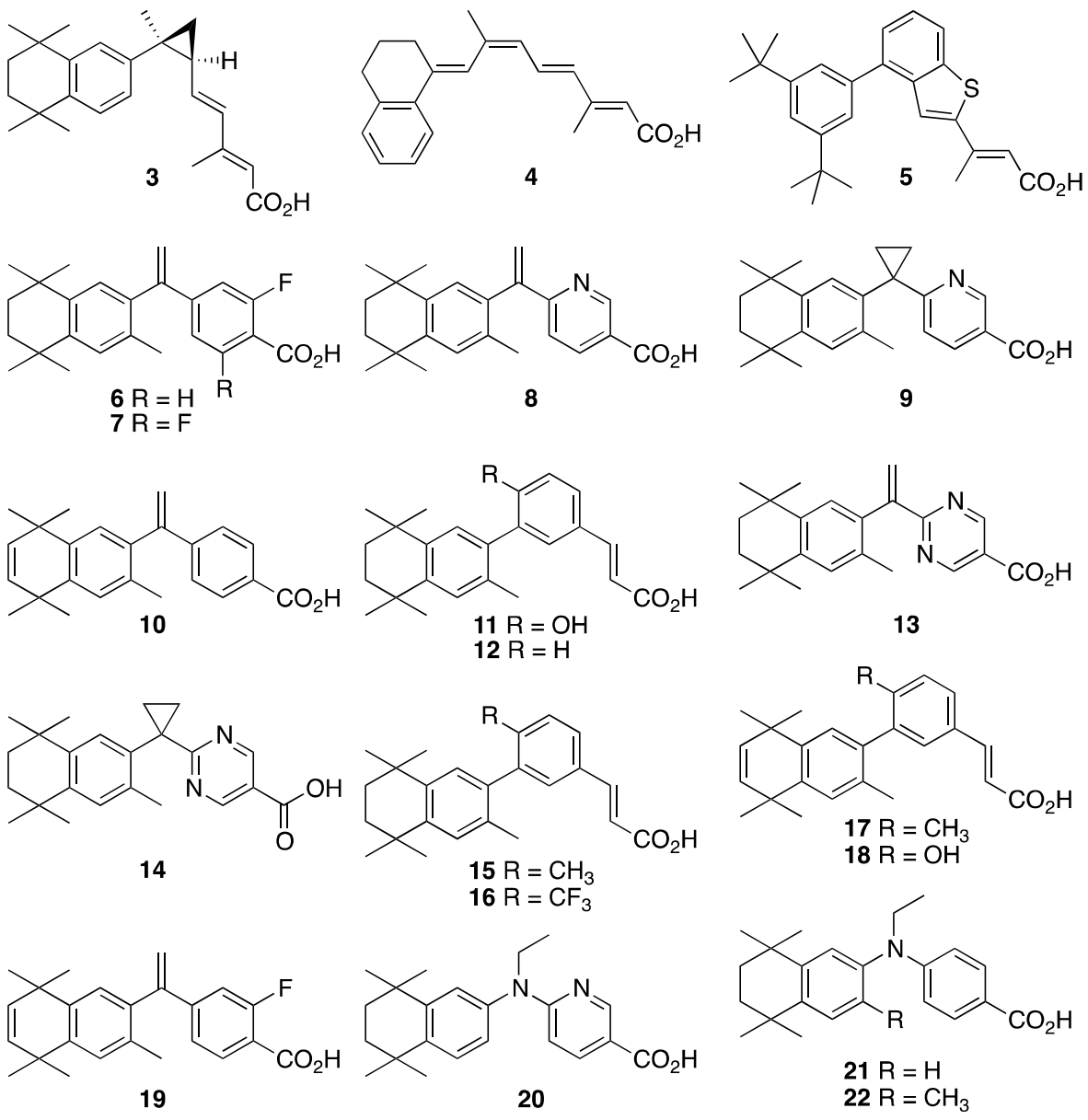

Figure 2. Additional synthetic rexinoids modeled after 9-*cis* retinoic acid.

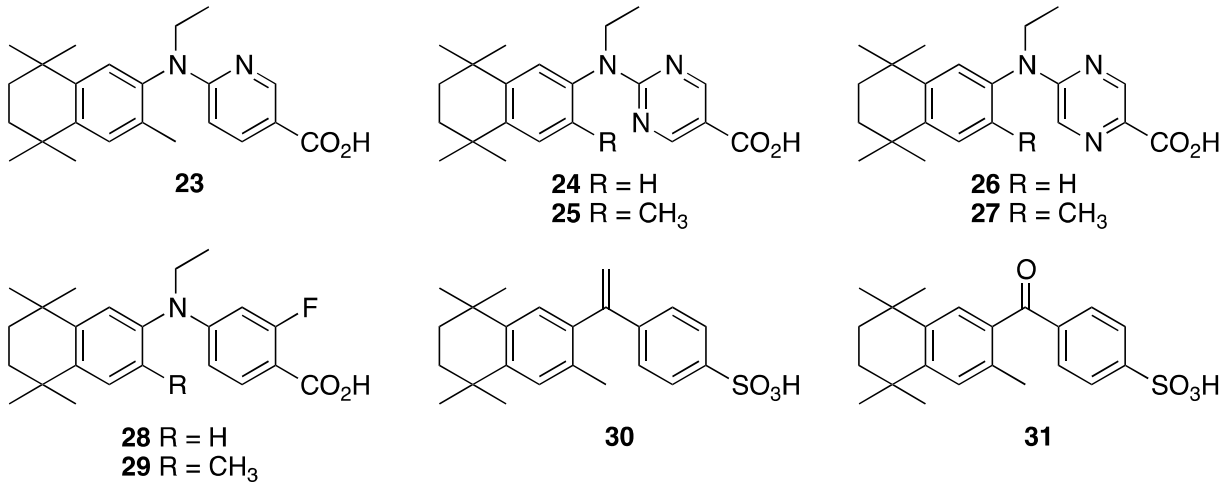

Figure 3. New rexinoids, **23-31**, prepared and evaluated in the present study.

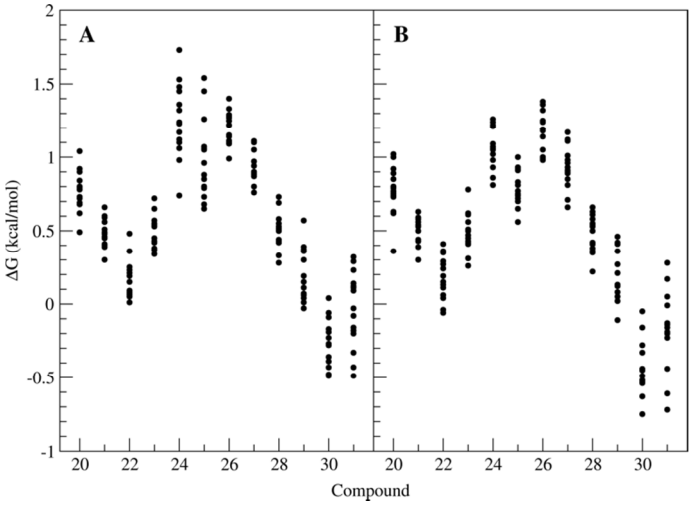

Figure 4. Docking results for compounds **20-31** relative to bexarotene. For each compound and for bexarotene, docking was performed to fifteen different RXR ligand binding domain structures. Each circle represents the difference in binding free energy between the best pose of the compound and the best pose of bexarotene in one of the RXR structures; negative values indicate better binding than bexarotene. A) Autodock charges. B) OpenBabel charges.

Figure 5

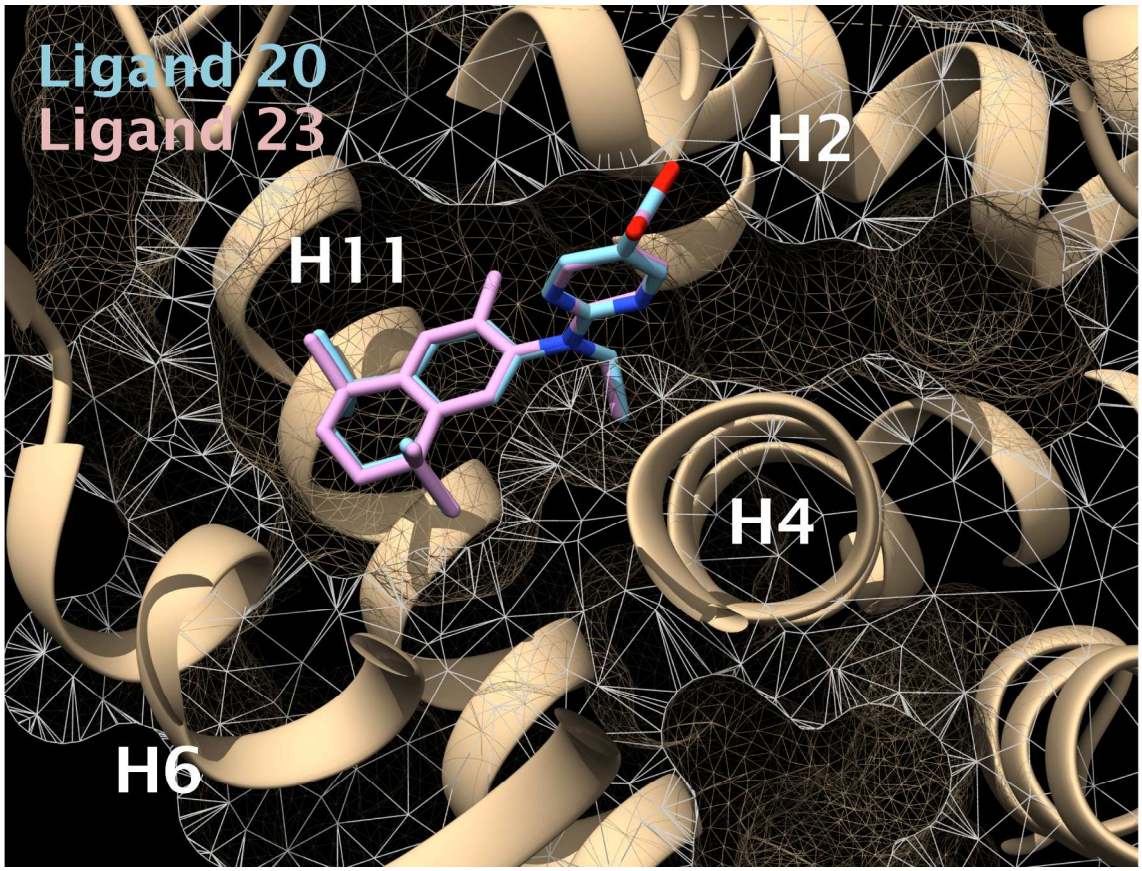

Figure 5. Top poses for **20** (blue) and **23** (violet) docked to the RXR binding pocket.

Scheme 1

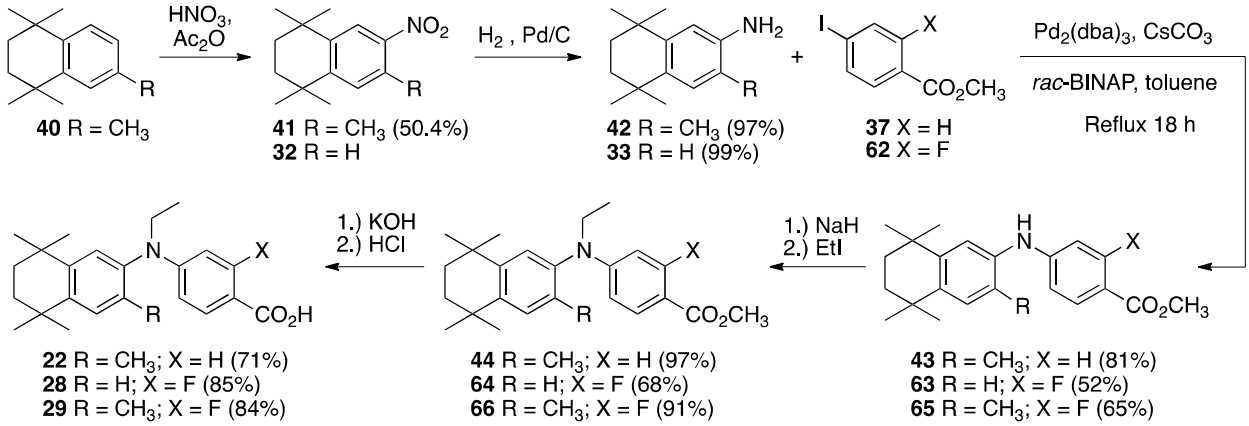

Scheme 1. Shared synthetic route for compounds **22**, **28**, and **29**.

Scheme 2

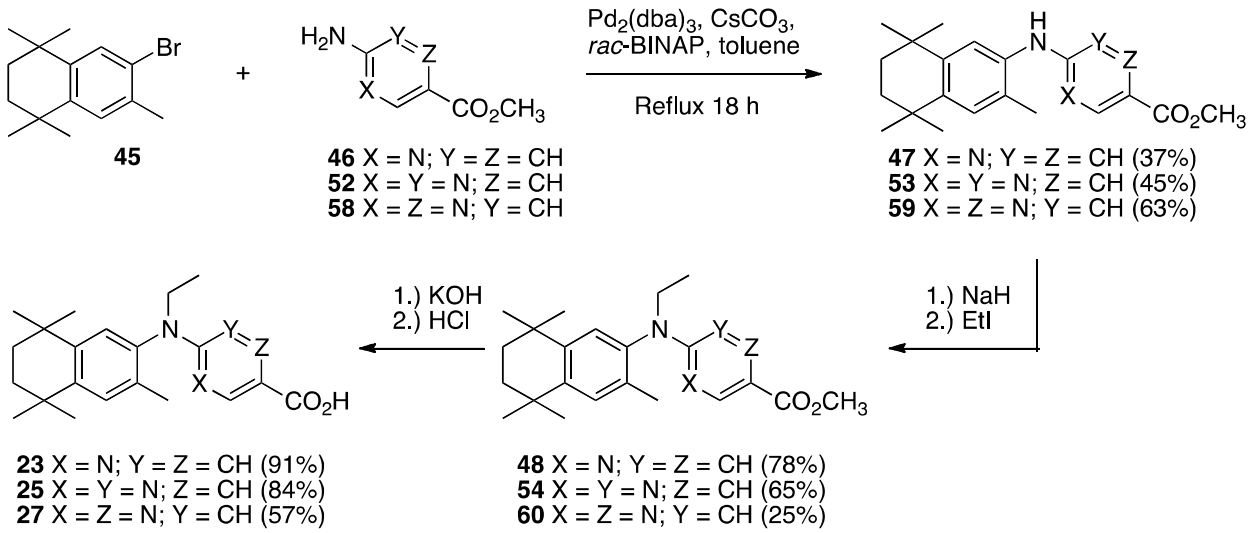

Scheme 2. Shared synthetic route for compounds **23**, **25**, and **27**.

Scheme 3

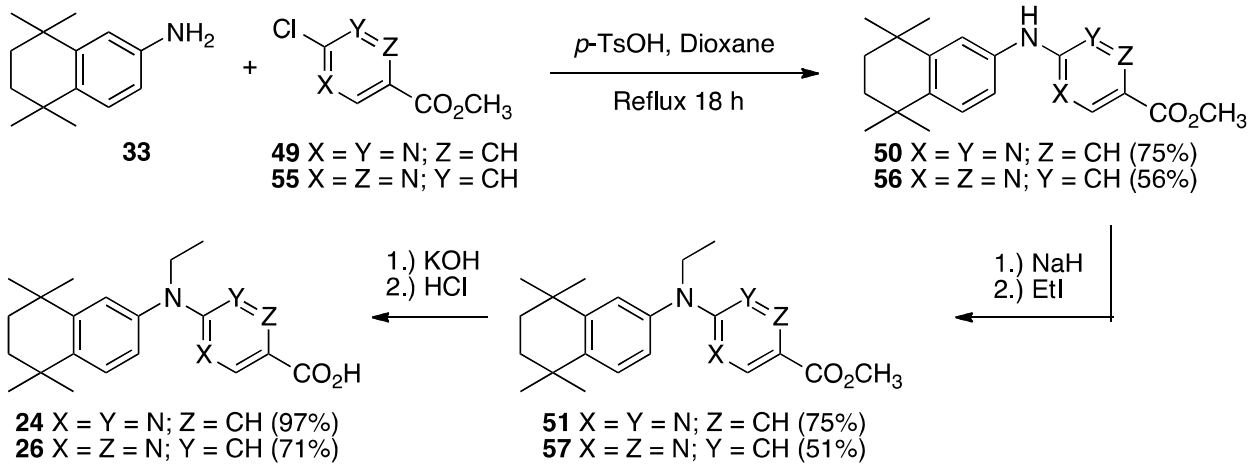

Scheme 3. Shared synthetic route for compounds **24** and **26**.

Scheme 4

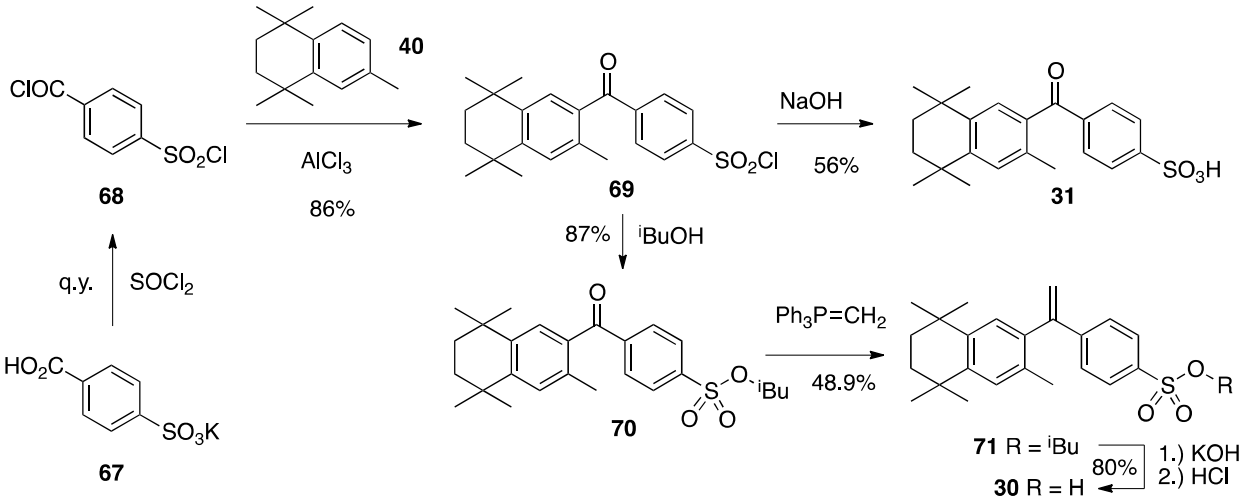

Scheme 4. Synthetic route to sulfonic acid bexarotene analogs **30** and **31**.

Figure 6

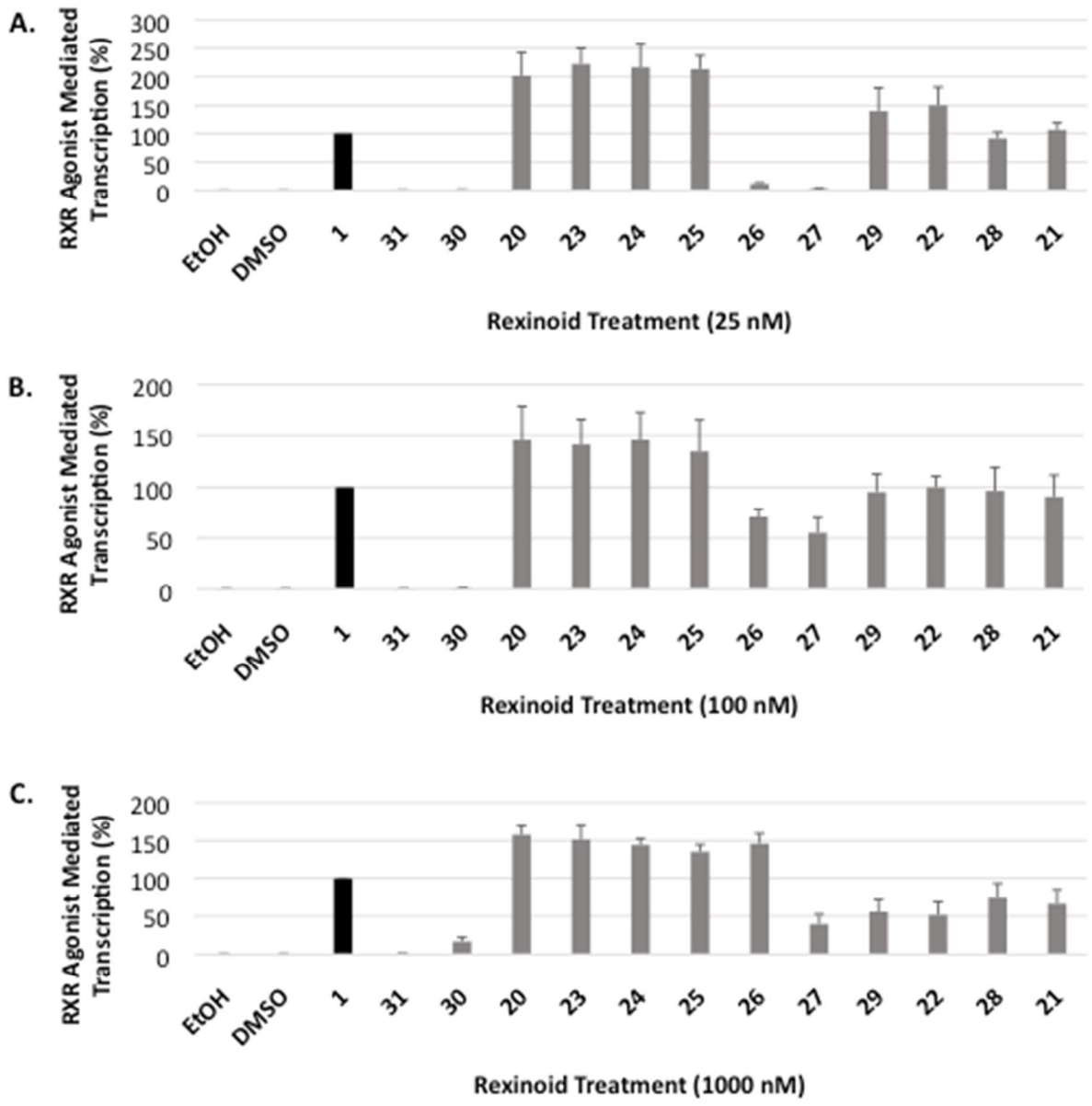

Figure 6. Identification of RXR agonists via a mammalian two-hybrid screening assay in human colon cancer cells. HCT-116 human colon cancer cells were cotransfected using pCMV-hRXR binding domain vector (BD) and pCMV-hRXR activation domain (AD) with pFR-Luc reporter gene containing BD-binding sites, and renilla control plasmid. Cells were transfected for 24 hours utilizing a liposome-mediated transfection protocol and then treated with either ethanol or DMSO vehicle, or analogs at 25 nM **(A)**, 100 nM **(B)**, 1000 nM **(C)** for 24 hours. Analog-mediated RXR binding and homodimerization, as measured by luciferase output, was compared to RXR agonist parent compound **1**, set to 100%.

Table 1: Determination of EC_{50} Value in the RXR Mammalian Two-Hybrid Assay

Compound	EC_{50} Value nM (SD)	Compound	EC_{50} Value nM (SD)
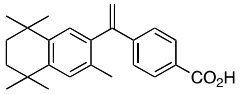 **1**	52.0 (2.1)	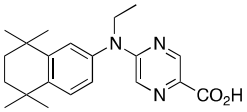 **26**	364.3 (3.7)
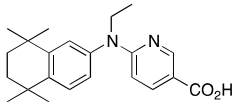 **20**	13.8 (0.8)	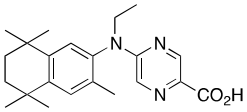 **27**	295.5 (0.8)
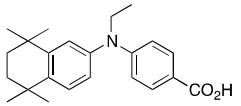 **21**	143.4 (1.6)	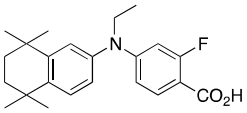 **28**	125.6 (2.3)
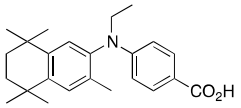 **22**	7.9 (0.4)	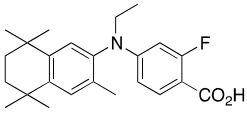 **29**	33.8 (0.1)
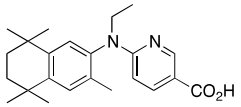 **23**	13.8 (1.5)	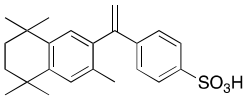 **30**	18,200 (250)
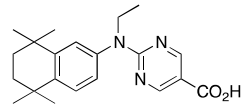 **24**	40.9 (0.6)	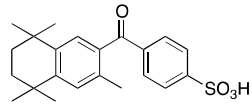 **31**	> 80,000
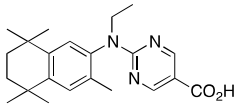 **25**	18.2 (0.4)		

Figure 7

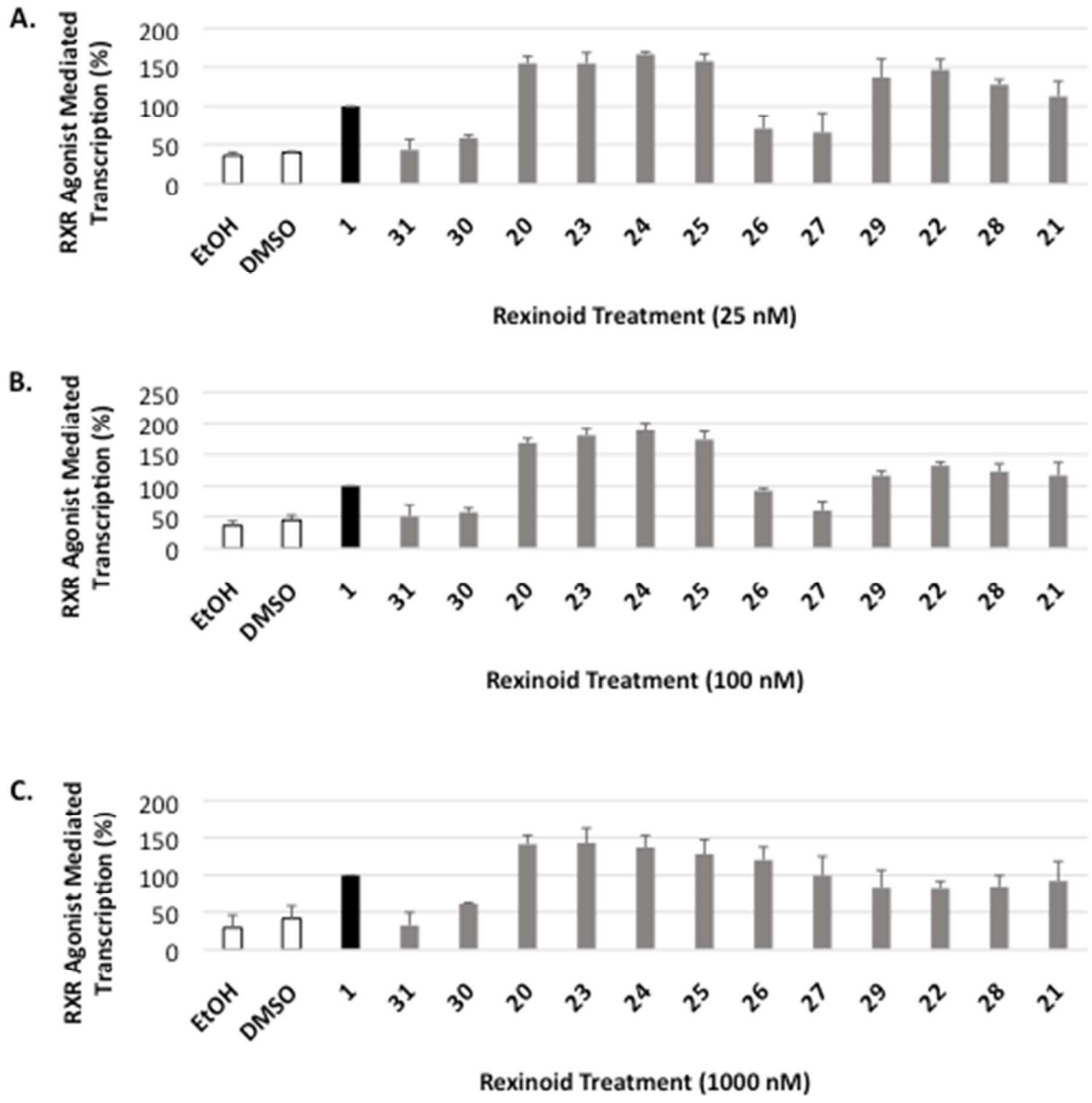

Figure 7. Evaluation of RXR agonists via an RXRE-luciferase reporter-based assay in human colon cancer cells. HCT-116 human colon cancer cells were transfected with a human RXRα expression vector, an RXRE-luciferase reporter gene, and a renilla control plasmid. Cells were transfected for 24 hours utilizing a liposome-mediated transfection protocol and then treated with either ethanol or DMSO vehicle, or analogs at 25 nM **(A)**, 100 nM **(B)**, 1000 nM **(C)** for 24 hours. RXR-mediated transcription, as measured by luciferase output, was compared to the parent compound **1**, set to 100%.

Figure 8

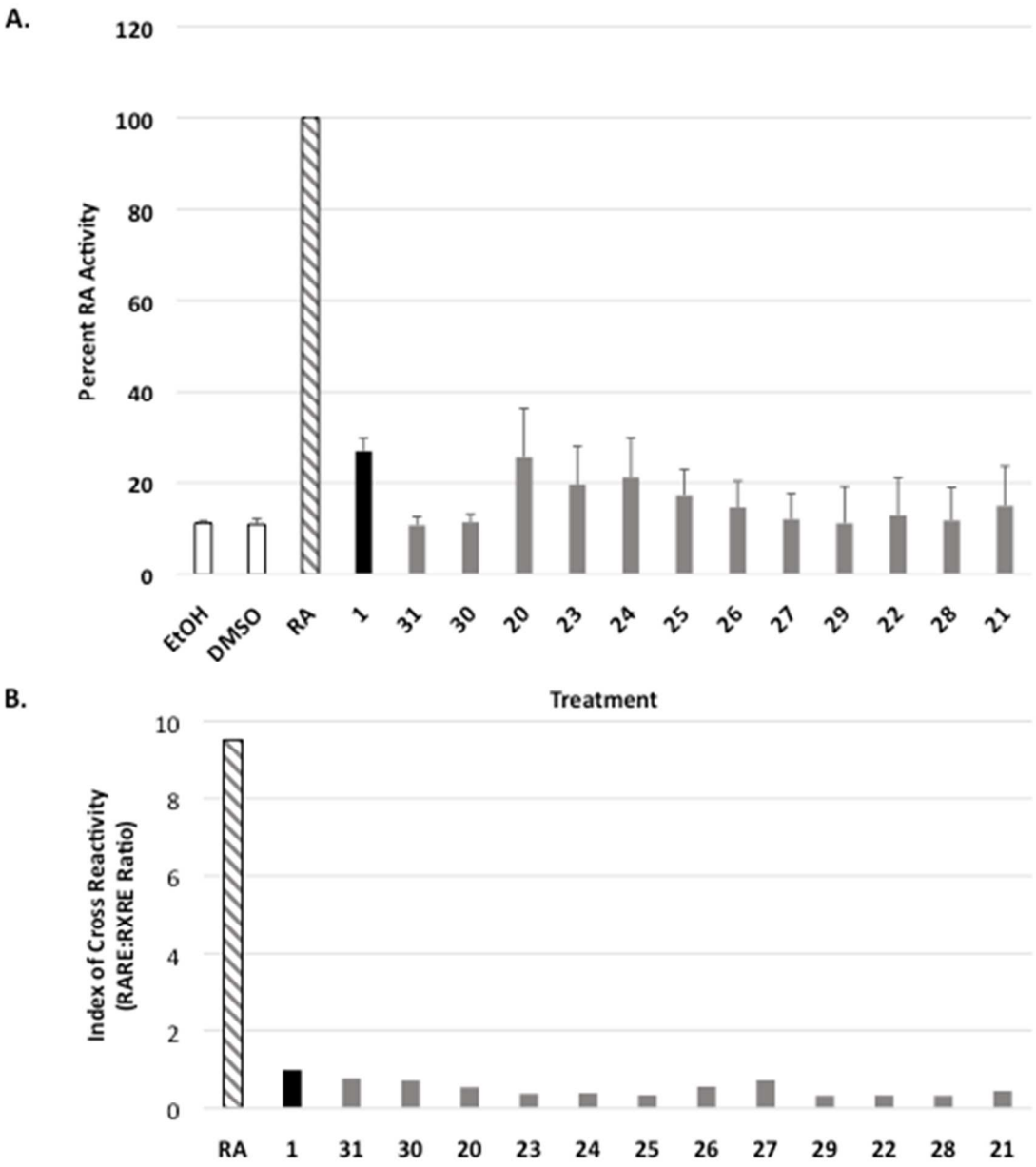

Figure 8. Assessment of RXR agonists via an RARE-luciferase reporter based assay in human kidney cells. **A)** Human embryonic kidney cells, HEK293, were co-transfected with expression vectors for hRXRα, hRAR, a RARE-luciferase reporter gene, and a renilla control plasmid for 24 hours utilizing a liposome-mediated transfection protocol. Cells were treated with analog or all-*trans*-retinoic acid (RA) at 100 nM for 24 hours. The RARE activity for RA is set to 100%. **B)** The "Index of Cross Reactivity" was determined by the RARE:RXRE ratio activity with Compound **1** set to 1.0.

Figure 9

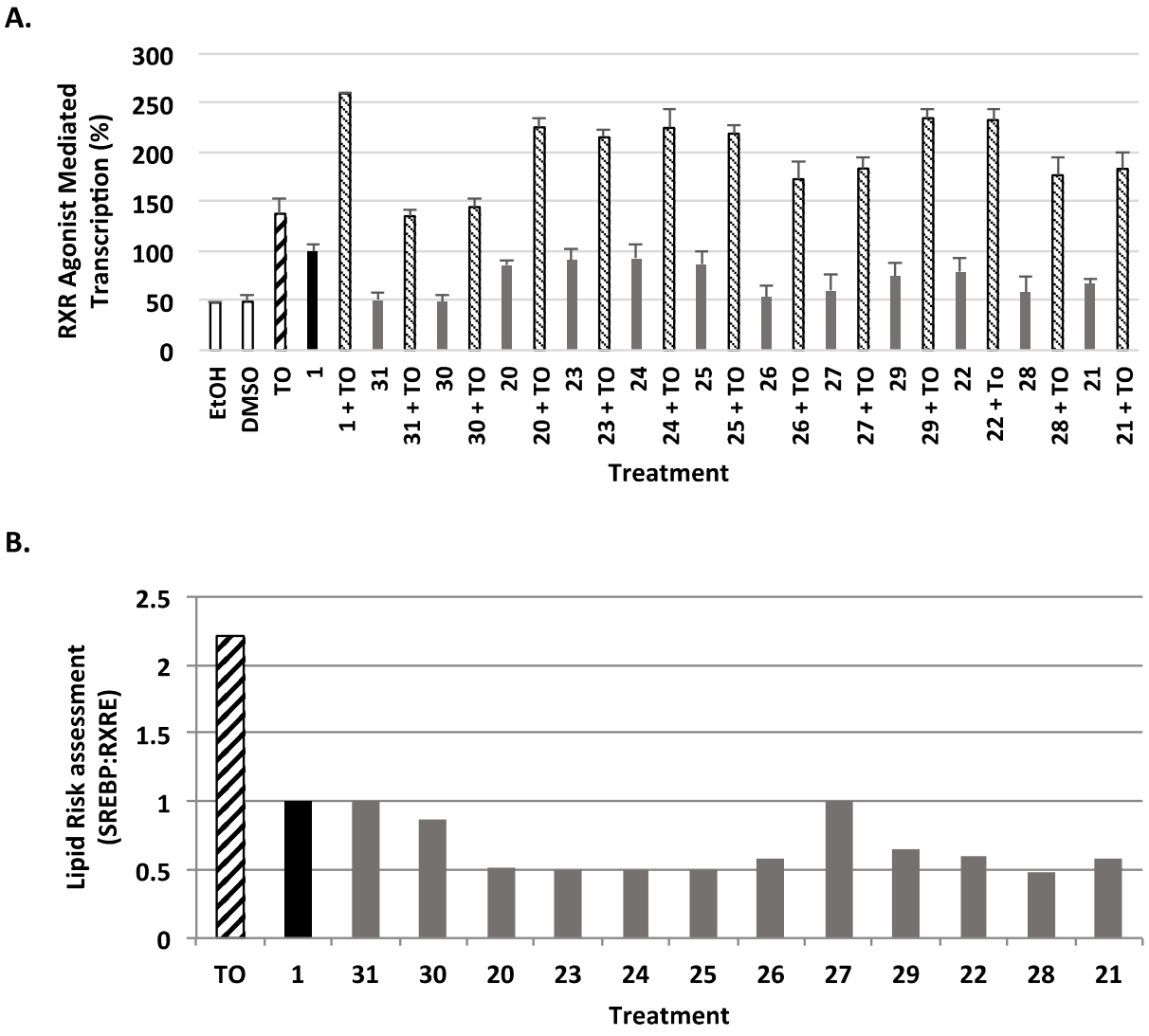

Figure 9. Evaluation of RXR agonists to potentiate SREBP promoter activation in the absence and presence of LXR ligand T0901317. A) HCT-116 human colon cancer cells were transfected with an expression vector for human LXRα, an SREBP-promoter-luciferase reporter gene, and a renilla control plasmid. Cells were transfected for 24 hours utilizing a liposome-mediated transfection protocol and then treated with ethanol or DMSO vehicle, or 100 nM of the indicated compound alone or in combination with 100 nM TO901317 (TO). SREBP promoter-directed activity was compared to compound 1, set to 100%. **B)** The "Lipid Risk Assessment" was determined by the SREBP:RXRE ratio with compound **1** set to 1.0.

Figure 10

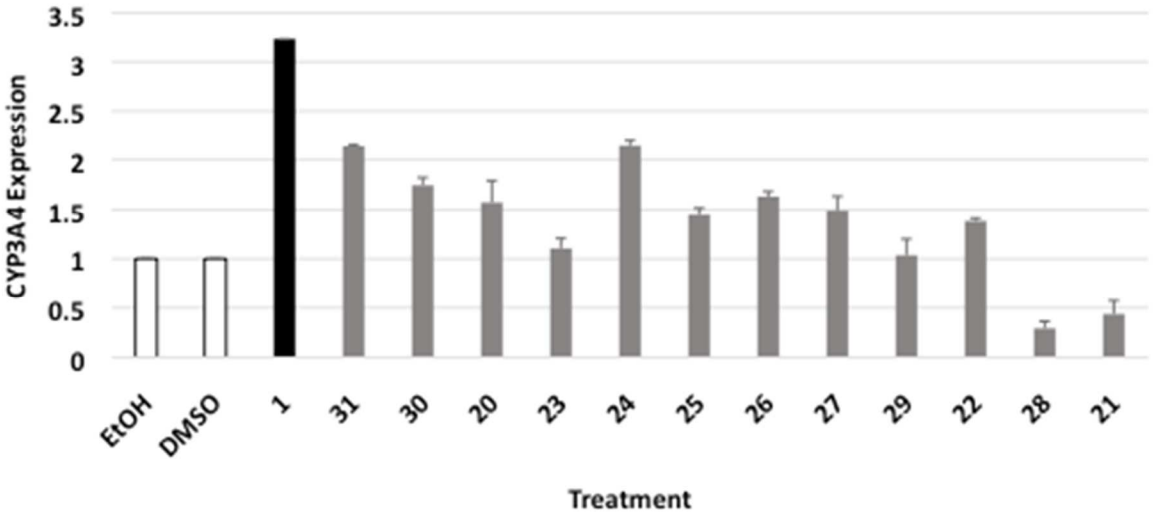

Figure 10. Assessment of RXR agonists to induce CYP3A4 expression. Human hepatocellular carcinoma cells (HepG2) cells were treated for 24 hours with ethanol or DMSO vehicle, or 100 nM of the indicated compound. Total RNA was extracted and 0.5 µg of DNase-treated sample was used for cDNA synthesis and subsequent qPCR. Data analysis was performed using the comparative ΔΔCt method as the means of relative quantitation, normalized to an endogenous reference (GAPDH) and relative to a calibrator (normalized Ct value from vehicle-treated cells) and expressed as $2^{-\Delta\Delta Ct}$. Ethanol and DMSO are set to 1.0.

Figure 11

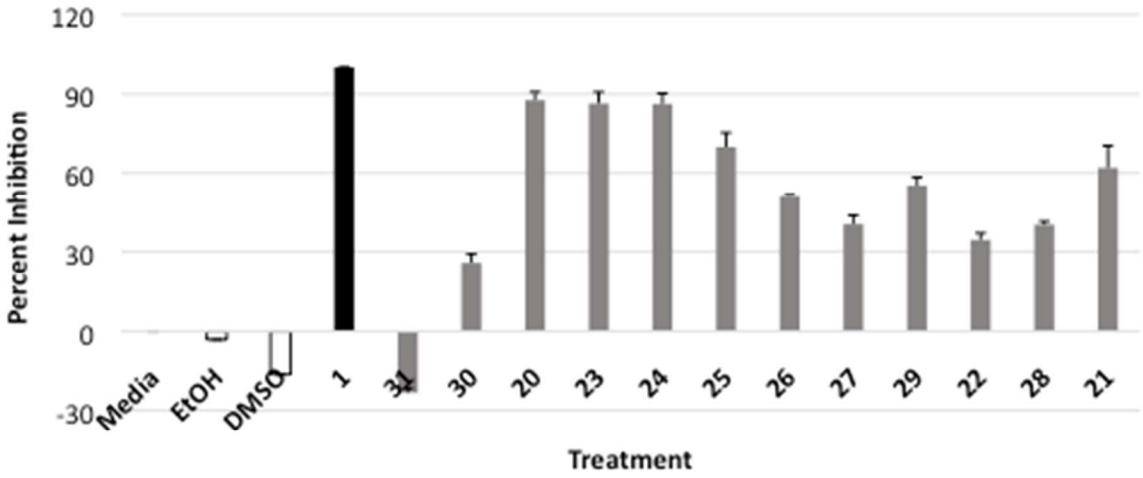

Figure 11. Probing of compound 1 and select analogs for inhibition of cell growth utilizing a MTS assay in CTCL. Human cutaneous T-cell lymphoma (Hut78) cells were plated at 7500 cells per well and immediately dosed with 200 nM of either ethanol or DMSO vehicle, or the indicated analog for 72 hours. RXR-mediated inhibition of growth was compared to compound **1**, set to 100%. The data represent an average of three independent experiments.

Figure 12

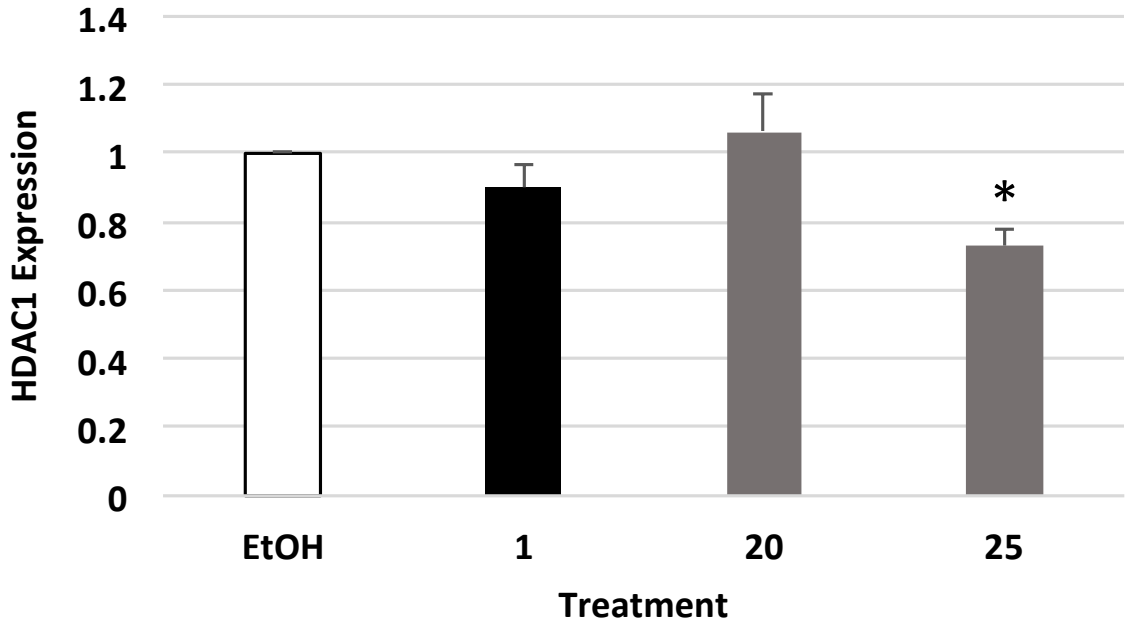

Figure 12. Ability of RXR agonists to repress HDAC-1 expression. Human cutaneous T-cell lymphoma (Hut78) cells were treated for 48 hours with ethanol or 100 nM of the indicated compound. A 0.5 µg portion of DNase-treated RNA was used for cDNA synthesis and subsequent qPCR. Data analysis was performed using the comparative ΔΔCt method as the means of relative quantitation, normalized to an endogenous reference (GAPDH) and relative to a calibrator (normalized Ct value from vehicle-treated cells) and expressed as $2^{-\Delta\Delta Ct}$. Ethanol is set to 1.0. * indicates $p < 0.05$ versus compound **1** utilizing an unpaired homoscedastic Student's T-test.

Table of Contents Graphic